공학박사 학위논문

기상냉매 주입 기술을 고려한 자동차 용 열펌프의 성능향상에 대한 연구

Studies on the Performance Enhancement of an Automotive Heat Pump System Considering Vapor Injection Technique

2015년 2월

서울대학교 대학원

기계항공공학부

김 모 세

Abstract

Studies on the Performance Enhancement of an Automotive Heat Pump System Considering Vapor Injection Technique

Mo Se Kim
Department of Mechanical and Aerospace Engineering
The Graduate School
Seoul National University

Recently, efficiency of energy consumption and side effects which is caused by synthetic refrigerant become more important. In this situation, electric vehicle is expected as a promising transport method in next generation. However, electric vehicle cannot supply excessive heat to cabin room as heating solution and extra heating apparatus should be used. Simple electric heater consumes much of energy to generate heat while heat pump can generate more heat than the consumed electricity. In this reason heat pump is expected to be used in electric vehicle. However, the

limitation of size for mobile application causes insufficiency of swept volume of compressor and some special method is required to increase heat capacity in vehicle heat pump system. Vapor injection technique is one of the popular technique of enhancing heat capacity but the most of the studies on it is for residential or commercial application. In this study vapor injection technique for vehicle heat pump system was investigated. The characteristics of vehicle heat pump system were considered. Important design factors and steady state system response which is related with control problem were analyzed experimentally and numerically. It was showed that one should consider compressor pressure control and injection amount in the control strategy. Additionally, on-line optimal control strategy for CO_2 refrigeration system was investigated. CO_2 is one of environmentally benign refrigerant but it forms trans-critical system when it is applied to general refrigeration system. Hence, it causes problem of determining optimal heat rejection pressure and it is one of the important issues of using CO_2 refrigeration system. In this study, assuming ideal refrigeration system, ratio of cooling capacity increment to work increment was estimated and comparing this with present COP, new on-line optimal efficiency control method was devised. This method does

not require precedence experimental correlations. The validity of the control method was verified experimentally and some causes of inducing performance degrade were analyzed. These studies are expected to be helpful for using energy in more efficient way and protect the environment.

Keywords: Heat pump, Vapor injection technique, CO_2, Efficiency control, Heat capacity

***Identification Number*: 2010-30791**

Contents

List of Figures

List of Tables

Nomenclature

COP	coefficient of performance
DSC	degree of subcool [K]
DSH	degree of superheat [K]
P	Pressure [kPa]
T	temperature [K]
UA	overall heat transfer coefficient [J/m^2s]
$\dot{W}$	work rate [kW]
$\dot{Q}$	heat rate [kW]
a	basic circle radius
h	enthalpy [$kJkg^{-1}$]
$\dot{m}$	mass flow rate [kgs^{-1}]
r	radius
t	involute angle
$\dot{w}$	specific work rate [kW/kg]
θ	angle

Subscript

air	airside
cond	condenser
dis	discharge
dum	dummy variable
gc	gas-cooler
heat	heating

IHX	internal heat exchanger
in	inlet
low	low pressure side
out	outlet
rear	rear side
front	front side
sat	saturation
suc	suction
vap	vapor

Chapter 1. Introduction

1.1 Background of the study

Recently, global warming effect has risen as a one of severe environmental problems and people are interested in developing technique which can prevent global warming effect. In refrigeration fields, one of the major efforts to prevent the global warming is making the system efficiency higher and to use of low global warming potential refrigerant. By making a system efficiency higher, energy consumption is reduced and corresponding CO_2 emission is decreased. In this background, vapor injection technique can be suggested as one of the techniques which help reducing energy consumption. Vapor injection is well-known technique which has been used for enhancing performance of heat pump but the approaches in academic aspects are not sufficient and to comprehend vapor injection system, more investigation is required still yet.

In this study, a heat pump which adopts vapor injection technique is investigated in electric car system. Electric car is one of the most promising transport methods which has high efficiency and does not emit any pollutants. However, it has some significant weak point that the battery used in an electric car does not provide sufficient energy to cover sufficient driving range. Moreover, an electric vehicle should be equipped with appropriate cooling and heating method for cabin passengers and driving range gets shorter as the cooling or heating apparatus. Between two of them, generally heating

apparatus consumes more electric energy and makes driving range shorter. Hence, vapor injection technique for a heat pump in winter season is studied in this study.

Also, CO_2 refrigeration system is also studied in this study for the purpose of reducing global warming. CO_2 is one of the natural refrigerants which has negligible global warming potential compared to conventional synthetic refrigerant. It also possesses acceptable thermo-physical properties as refrigerant. However, in a CO_2 refrigeration system, there exists some peculiar characteristics which makes the CO_2 system distinguishable to the conventional system. The most distinct characteristic is that it forms trans-critical cycle in general refrigeration conditions. Because of the low critical temperature of CO_2, the heat rejection pressure of CO_2 refrigeration should be higher than the critical pressure and heat is released in super-critical state with continuous temperature glide. Hence heat rejection pressure moves widely and corresponding system performance also varies significantly. As a result, controlling heat rejection pressure is one of the very important issues in using CO_2 refrigeration system and this subject is treated in this study.

1.2 Introduction to Vapor Injection Technique

Vapor injection technique is one of the popular techniques which are used to obtain extra heat capacity by heat pump. Displacement of a compressor is fixed and the maximum refrigerant mass flow rate decreases when outdoor temperature is too low. Hence, most of heat pumps are not capable of supplying sufficient heat in cold winter season. Recently, much of heat pump manufacturers adopt vapor injection technique to overcome the lack of heat capacity in cold temperature conditions. Especially, density of R134a in saturated vapor state easily decreases as temperature goes low. In this reason, a heat pump system which uses R134a shows significant degrade in heating capacity with decrement of outdoor temperature and importance of using vapor injection technique is more emphasized.

Using a vapor injection compressor for which additional vapor refrigerant is injected into the vapor injection hole separated from suction process. The compressor transport more vapor refrigerant into condenser and heat capacity can be increased. The supplying of vapor refrigerant can be achieved by using an internal heat exchanger or flash tank. Both type of vapor injection technique are bounded in the limit that amount of refrigerant which flows through evaporator does not vary and increment of heat capacity is originated from decrement of enthalpy decrease of refrigerant at evaporator inlet. The amount of generated vapor refrigerant is also bounded by this limit. Hence, the limitations and characteristics of vapor injection technique should

be investigated to establish control method and design a system appropriately. This study will provide useful information with regard to the characteristics of vapor injection technique which is applied to vehicle heat pump system in experimentally and analytically. It is expected that this information helps the development of the technology.

1.3. Introduction to CO_2 Refrigeration System

CO_2 is one of the traditional natural refrigerant which is used at early stage of this century. However, using of CO_2 as refrigerant almost has disappeared until recently because of relatively high operation pressure compared to the synthetic refrigerants. However, environmental problem has deteriorated in recent years and the problems which are caused by synthetic refrigerant also arise to big issues. The most well known problems are ozone depletion problem and global warming problem and compared to synthetic refrigerant, CO_2 refrigerant causes almost negligible global warming problem and no ozone depletion problem. This is the most important virtue of using CO_2 as refrigerant. Very low GWP (Global Warming Potential) and 0 ODP (Ozone Depletion Potential). HCFCs and CFCs which are developed to replace high ODP refrigerants have much higher GWP compared to CO_2 for time horizons of 20, 100 and 500 years. GWPs calculated for different time horizons show the effects of atmospheric lifetimes of each refrigerant.

Another distinguishable feature of a refrigeration system which uses CO_2 refrigerant are that the cycle forms trans-critical cycle and the pressure of the

system is relatively high compared to the conventional systems. Critical pressure of CO_2 is relatively high and critical temperature is relatively low to the other conventional refrigerants. Hence, general operating situation of CO_2 refrigeration system contains super critical heat rejection process especially in high ambient operating conditions.

The volumetric refrigeration capacity of CO_2 is much superior to the other refrigerants and this factor makes the volume of the system be smaller compared to the conventional refrigeration system. Large specific heat and thermal conductivity improve heat exchanger performance and these properties can be regarded as advantages of using CO_2 refrigerant.

The cycle of CO_2 refrigeration system consists of compression, heat rejection, expansion and heat absorption process. All the other processes are very similar with cycle processes of conventional refrigeration system except heat rejection process. Heat rejection process of CO_2 refrigeration system is called as gas-cooling process and during the process, single phase of gas like refrigerant is cooled down to liquid like state refrigerant with large temperature glide. In this reason, the system cannot reject much heat during heat rejection process because of relatively low critical temperature. To overcome this weak point, an internal heat exchanger is usually used for CO_2 refrigeration system. However, the super critical heat rejection process and adopting of an internal heat exchanger causes significant problem in control aspect. In conventional system, one can regulate heat rejection pressure by using liquid receiver but it is impossible for CO_2 refrigeration system. The internal heat exchanger also generate expansion valve control problem

because it removes an important indicant which is DSH at evaporator outlet. Hence, for a CO_2 refrigeration system, heat rejection pressure becomes a very important indicant to control expansion valve opening and resulting COP. In this study, a method to determine optimized heat rejection pressure is suggested and its and limitations and validity will be discussed.

Chapter 2. Experimental Study on the Performance Improvement of a Heat Pump Using Vapor Injection Technique

2.1 Introduction

Recently many of heat pumps which are used in winter season start to adopt vapor injection technique to enhance heating performance. Vapor injection technique is basically to inject some extra portion of vapor refrigerant into compressor separately from normal suction refrigerant. To accomplish vapor injection the system should make extra vapor refrigerant and an internal heat exchanger or a phase separator is generally used for this purpose (Fig. 2.1). Then, the injected extra vapor refrigerant surely has heating potential and the system can provide more heat to the target.

In this study, a heat pump using vapor injection technique which uses an internal heat exchanger will be investigated and the schematic of a vapor injection heat pump using an internal heat exchanger is presented in Fig. 2.1 (a). According to the figure, the stream of refrigerant which flows out at condenser outlet is divided into two separate streams. One of the streams is

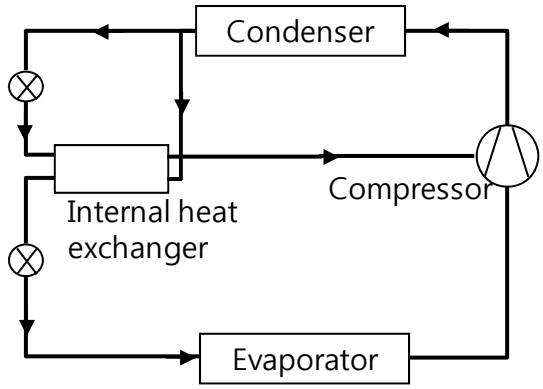

(a) Internal heat exchanger vapor injection cycle

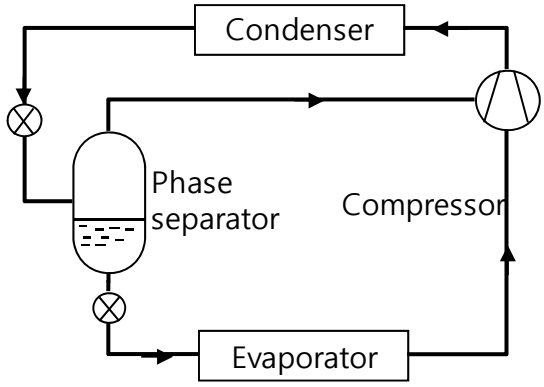

(b) Phase separator vapor injection cycle

Fig. 2.1 Schematics of vapor injection cycle using an internal heat exchanger and phase separator

expanded and becomes two-phase state (Fig. 2.2) and its temperature reduces. Then, this low temperature two-phase stream and the other stream which is non-expanded and maintains its state as it flows out at condenser start to exchange heat to each other. As a result of the heat transfer, the two-phase low temperature stream gains heat from the non-expanded stream and vaporizes while the non-expanded stream becomes cooler. In this process, the system can obtain extra vapor refrigerant and if the pressure of the expanded stream is higher than the evaporation pressure at evaporator, the system efficiency could be improved. In this reason, the vapor injection technique has attracted much of concerns and been used in many applications.

In practical use, the main purpose of using vapor injection technique is to obtain more heat capacity with limited compressor stroke volume. However, it is certain that there is limit to increase heat capacity using vapor injection technique. The phase separator using vapor injection heat pump system for example, cannot separate vapor and liquid if DSC at condenser is very low and this condition is presented in Fig. 2.3. Fig. 2.3 (a) represents the pressure-enthalpy diagram of phase separator vapor injection cycle when DSC is appropriate and Fig. 2.3 (b) represents the cycle state when DSC is fairly large. In the later case the refrigerant at condenser outlet does not

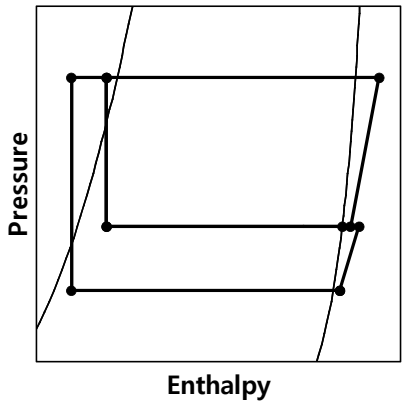

(a) Vapor injection cycle

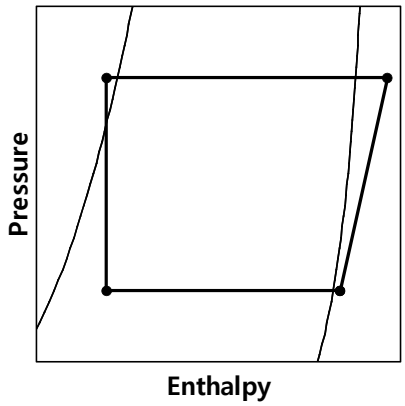

(b) Conventional cycle

Fig. 2.2 Pressure-enthalpy diagram of vapor injection cycle and conventional cycle

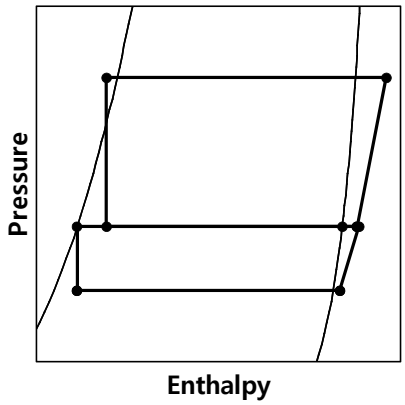

(a) Small DSC condition

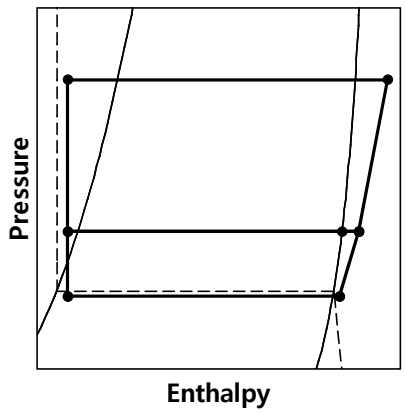

(b) Large DSC condition

Fig. 2.3 Pressure-enthalpy diagram of phase separator vapor injection cycle when DSC is small and large

become two-phase state although the pressure is dropped to fairly low pressure but even evaporator inlet refrigerant is almost liquid state. The dashed line in the figure represents isothermal line and one can see that if condenser outlet temperature goes down to near evaporation temperature, phase separator does not work at fairly low injection pressure. This excessively large DSC condition does not occur in general operating condition, but if condenser is relatively small compared to evaporator and the secondary fluid temperature at condenser and evaporator are the same when refrigerant flow is relatively small.

A vehicle heat pump system might meet with this condition. In winter season, the air temperatures in cabin and outdoor are the same temperature and it has small condenser compared to evaporator. Moreover, as stated in the previous chapter, specific density of R134a which is used for heat pump in vehicle becomes fairly large at low temperature condition resulting in insufficient transport of refrigerant by compressor. Hence, a study on the vapor injection heat pump for a vehicle should be carried out in different aspect from the aspect for residential vapor injection heat pump system. In this study, a heat pump system which is designed for electric vehicle is investigated to improve heating performance by using vapor injection technique with an internal heat exchanger. The most concerned condition is

start-up condition when the outdoor air temperature and cabin air temperature are the same. Passengers feel the strongest cold during start-up process and the largest heat is required while the refrigerant mass flow rate in the heat pump becomes deficient as outdoor temperature decreases. In the reason, the heating performance improvement in start-up condition is one of the important tasks to be assigned to the heat pump engineers.

2.2 Literature Review

Recently, heat pump is actively used as heating device during winter season, commercial heat pumps shows the trend of adopting vapor injection technique (Wang *et al*., 2009). Vapor injection technique is firstly introduced for room air conditioners (Winandy and Lebrun 2002; Xu *et al*. 2010) and now it is used in many commercial heat pumps. As stated, most of the vapor injection heat pumps using vapor injection technique which can be categorized by two types: flash tank using vapor injection (FTVI) technique and internal heat exchanger using vapor injection (IXVI) technique. The terminology ‘internal heat exchanger’ is sometimes called as ‘sub-cooler’. In their study, Wang *el al*. (2009) categorized recent studies on vapor injection technique into two categories: theoretical studies (Domanski (1995),

Vaisman (2000), Ma and Chai (2004), Siddharth *et al*. (2004)) and experimental studies (Zehnder *et al*. (2002), He *et al*. (2006), Bertsch and Groll (2008)). In theoretical studies, idealized model or simulation using investigations have been preformed. It is possible to reveal the potential performance enhancement of vapor injection by studying idealized vapor injection model. Detailed simulation model can give information about how one should design system dimension and how the control should be performed. By experimental studies, the validity of vapor injection technique was verified under various operational conditions and with some modified devices. In the above studies, R22, R507A, R404A, R407C, R134a and R410A were used. However, studies on vapor injection technique for application in electric vehicle were hardly found.

Nguyen *et al*. (2007) indicated that the IXVI cycle with thermostatic expansion valves had superior performance over a wide operating range to the FTVI cycle with capillary tube. Wang *et al*. (2009) also claimed that the IXVI cycle has wider operating range than the FTVI cycle. Xu *et al*. (2011) reviewed the studies on vapor injection technique and told that the control problem of vapor injection cycle is challenging issues and requires further investigations. Ma and Zhao (2008) showed the performance of a heat pump system having a flash tank

2.3 Experimental Apparatus and Data Reduction

The experimental apparatus consists of two-loops of wind tunnels and object vapor injection heat pump system. The two-loops of wind tunnels respectively simulate cabin-side environment and outside environment. Fig. 2.4 show the schematic of experimental apparatus and each wind tunnel equips temperature and humidity control chambers to control air temperature at front of the object heat exchangers. These object heat exchangers are condenser and evaporator and they are inserted respectively into the corresponding wind tunnel. The vapor injection heat pump system is set connecting with the condenser and evaporator. For simulating start-up condition of electric vehicle, indoor temperature and outdoor temperature are set to be the same. Each wind tunnel equipped with blower which places downstream of the heat exchanger. Before the blowers, flow meter for measuring air flow rate places.

Vapor injection heat pump system consists of a compressor, a condenser, an evaporator, an internal heat exchanger, a main expansion valve and an injection expansion valve. Schematic is presented in Fig. 2.1. A large evaporator and comparatively small condenser for electric vehicle are used

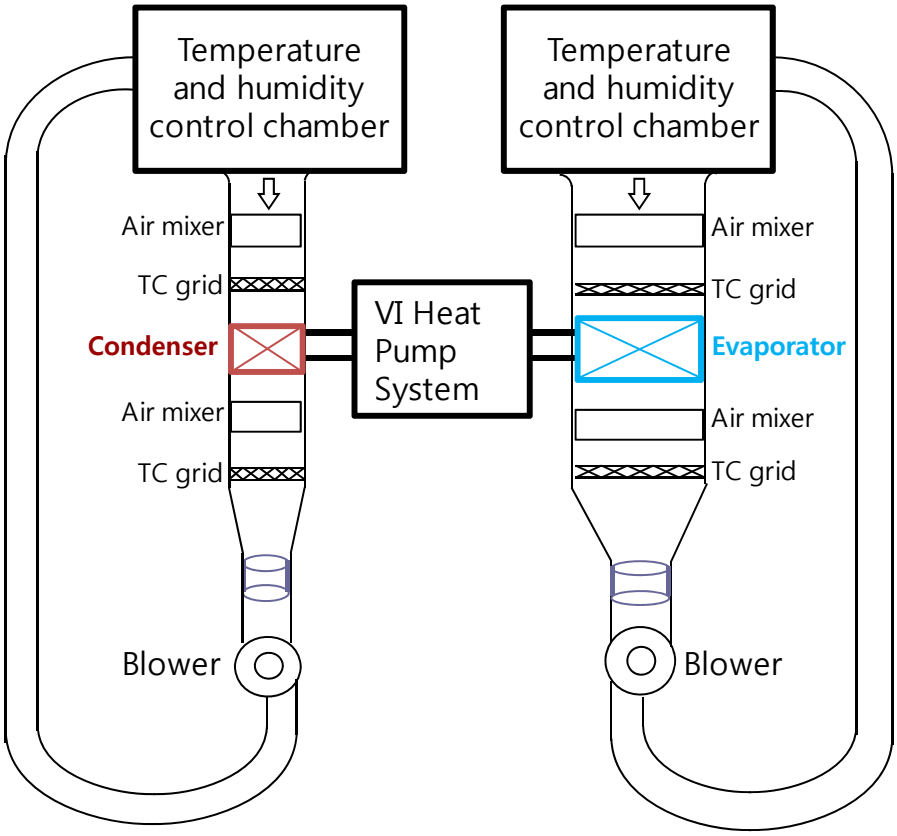

Fig. 2.4 Schematic of vapor injection heat pump system experimental apparatus

for the system. Each heat exchanger is plate tube-fin type heat exchanger and it the tube multi mini channels are manufactured with aluminum alloy. The width and height of condenser is about 200 mm and thickness is about 30 mm. Evaporator has width of about 1000 mm and height of about 600 mm with 30 mm of thickness. Plate type heat exchanger is used as an internal heat exchanger. More accurate dimensions of the system are kind of industrial secrets and cannot be revealed. Compressor is also selected as for electric vehicle heat pump system and modified as a vapor injection compressor.

Absolute pressures for each component are measured piezoelectric pressure sensors and differential pressure is also measured between inlet and outlet of each component. T-type thermocouples are inserted into the tubes and measured the bulk temperature of refrigerant at inlet and outlet of each component. Refrigerant mass flow rate was unable to obtain directly from mass flow meter because of characteristics of vapor injection compressor which generate fluctuation of refrigerant mass flow rate and calculated using energy balance (Eq. 2.1) at heat exchanger.

$$\dot{m}_{ref,cond}(h_{in,cond} - h_{out,cond}) = \dot{m}_{air,cond}(h_{air,rear,cond} - h_{air,front,cond}) \quad (2.1)$$

Referring to Ashrae standard 41.2-1987 (RA 92), nozzle type flow meter was used to measure air flow rate. Equally spacing 25 mesh grids are

made with thin string and 25 T-type thermo couples are placed at each cross point. Air mixers made by instruction of Ashrae standard 41.1-1986 (RA 2006) are used to remove temperature difference inside the duct.

$$\dot{Q}_{heat} = \dot{m}_{air,cond}(h_{air,rear,cond} - h_{air,front,cond}) \tag{2.2}$$

WT130 power meter manufactured by Yokogawa is used to measure consumed power at compressor and COP is calculated using Eq. 2.3.

$$\mathrm{COP}_{heat} = \frac{\dot{Q}_{heat}}{\dot{W}} \tag{2.3}$$

Required thermo-physical properties are obtained by Refprop 8.0 program by NIST and test conditions are presented by Table 2.1.

2.4 Experimental Results and Discussion

2.4.1 Effect of Vapor Injection on Heating capacity and COP

In the vapor injection study, the most concerned subject is about increase of heating capacity and COP. Fig. 2.5 shows how heating capacity varies as expansion valve opening in injection line increases. According to the figure, it is observed that heating capacity increases corresponding to large opening of injection line expansion valve expect when main expansion valve throat

Table 2.1 Experimental conditions

Parameters	Value
Compressor RPM	4500
Water flow rate (LPM)	18
Main expansion valve throat area (mm^2)	0.79, 0.66, 0.53, 0.40
Injection expansion valve throat area (mm^2)	0.0, 0.07, 0.13, 0.20
Refrigerant mass charge (g)	900, 1000, 1100
Indoor air temperature (°C)	-15
Outdoor air temperature (°C)	-15

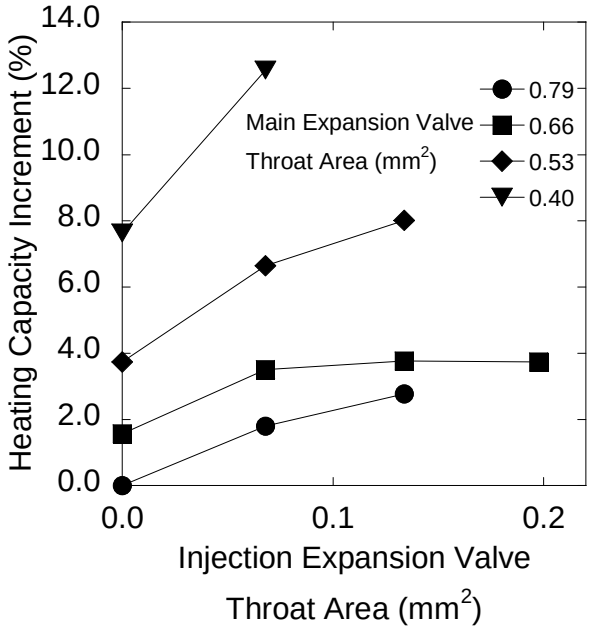

Fig. 2.5 Heating capacity change with respect to injection expansion valve opening and main expansion valve opening (m_{charge}: 1100 g)

area is 0.40 mm^2. At this time, the case in which main expansion valve throat area is 0.40 mm^2 will be ignored and treated later because this case shows some peculiar characteristics which is distinguishable from the other cases.

Except the stated special case, the increment of heating capacity is mainly due to the increment of mass flow rate caused by vapor injection. As vapor injection starts and injection expansion valve opening is increased, refrigerant mass flow rate in condenser becomes to increase due to the increased injected refrigerant mass flow rate. Fig. 2.6 shows this trend. However, when considering the specific enthalpy change of refrigerant between condenser inlet and outlet (Δh_{cond}) which is presented in Fig. 2.8, as amount of vapor injection increases, Δh_{cond} shows decreasing trend. This is because of the fixed condenser size while the mass flow rates increase. If increment of mass flow rate is comparatively large than increment of $UA\Delta T$ at condenser, Δh_{cond} should be decreased because $UA\Delta T_{cond} = \dot{m}_{cond}\,\Delta h_{cond}$. Hence, it is no wonder that the enthalpy differences between condenser inlet and outlet decreases.

With regard to main expansion valve opening, heating capacity generally increases as main expansion valve opening decreases. As closing the main expansion valve opening, condenser pressure is upraised and more efficient heat transfer is possible. This is one of the important characteristics of heat

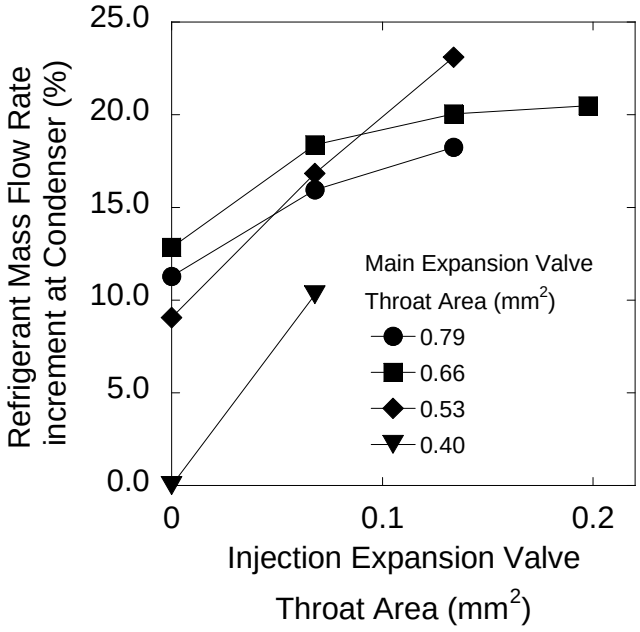

Fig. 2.6 Refrigerant mass flow rate change at condenser with respect to injection expansion valve throat area (m_{charge}: 1100 g)

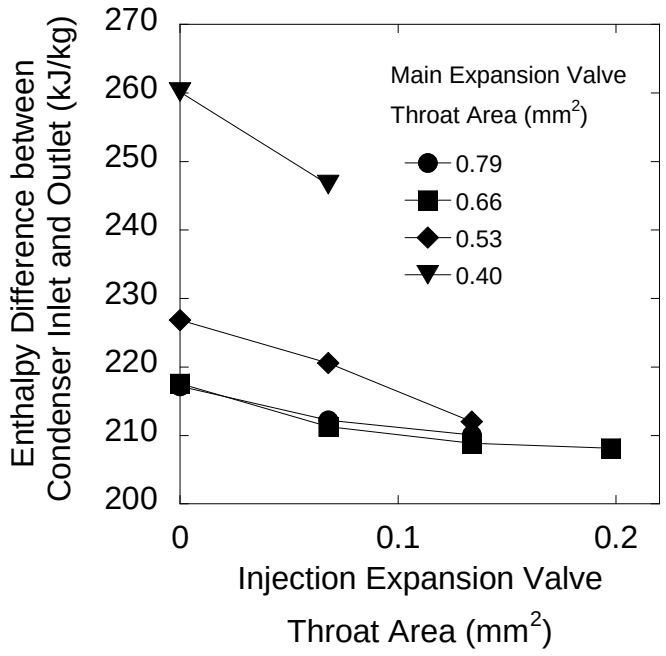

Fig. 2.7 Specific enthalpy difference between condenser inlet and outlet (m_{charge}: 1100 g)

pump for vehicle heat pump system. To reduce dependency on electric heater, it is important to enhance heat generation by heat pump system in electric vehicle. Although if the increment of heat capacity causes COP degrade, it is desirable to increase heat capacity and adopt smaller size of electric heater because of economic point of view.

Fig. 2.8 shows the typical pressure-enthalpy diagram of vapor injection cycle compared to conventional cycle. As stated above, the refrigerant enthalpy at condenser outlet slightly increases than that of the conventional cycle, but passing through the internal heat exchanger, evaporator inlet enthalpy becomes smaller than that of the conventional cycle. Hence, the refrigerant flows through evaporator can absorb more heat than that of the conventional cycle and heating capacity can be increased.

However, there is another important factor which increases heating capacity. Referring to Fig. 2.9, one can notice that the enthalpy at main expansion valve inlet does not fairly decrease compared to the no-injection heat pump cycle. This is not consistent with the forecast stated above with Fig. 2.2. According to the forecast, the enthalpy at expansion valve inlet should be decreased to absorb more heat at evaporator and satisfy the first law of thermodynamics. If the compressor stroke volume is fixed and density of refrigerant at compressor suction does not vary, the mass flow rate

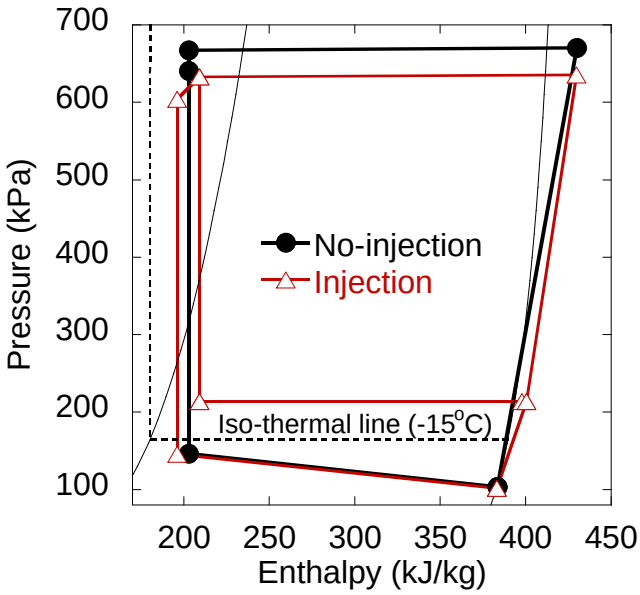

Fig. 2.8 Pressure-enthalpy diagram of no-injection heat pump and injection applied heat pump ($A_{throat,\ main}$: 0.53 mm^2, $A_{throat,\ inj}$: 0.07 mm^2, m_{charge}: 1100 g)

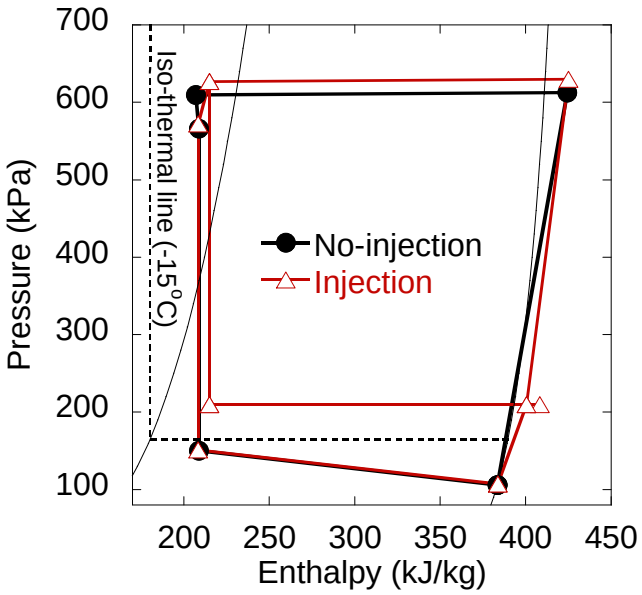

Fig. 2.9 Pressure-enthalpy diagram of no-injection heat pump and injection applied heat pump ($A_{throat,\ main}$: 0.79 mm^2, $A_{throat,\ inj}$: 0.13 mm^2, m_{charge}: 1100 g)

passing through evaporator also does not vary because the transferred mass from evaporator to higher pressure part is constant. In this reason, if only evaporator heat absorption is considered, heating capacity does not increase though mass flow rate passing through condenser increases. However, as vapor injection is performed, compressor work also should be considered. The refrigerant mass flow rate which enters at compressor suction port does not vary while vapor injection is performed, but the injected vapor consumes more work to be pressurized from injected pressure to compressor discharge pressure, compressor work becomes to be increased. The increased work makes the refrigerant at compressor discharge port be capable of having more heating potential and heating capacity can be increased finally.

In the stated case, it should be noted that the increased heat is directly obtained from compressor work and energy efficiency of the system must be decreased. Fig. 2.10 represents the COP of the vapor injection cycle with respect to change of injection expansion valve opening. The figure shows that the most of the COP of vapor injection cycle decreases as injection expansion valve opening increases except the case in which main expansion valve opening is very small. The existence of the exception case is caused because a system like that is represented by Fig. 2.8 also obtains extra heat from compression work in addition to the absorbed heat at evaporator. If the

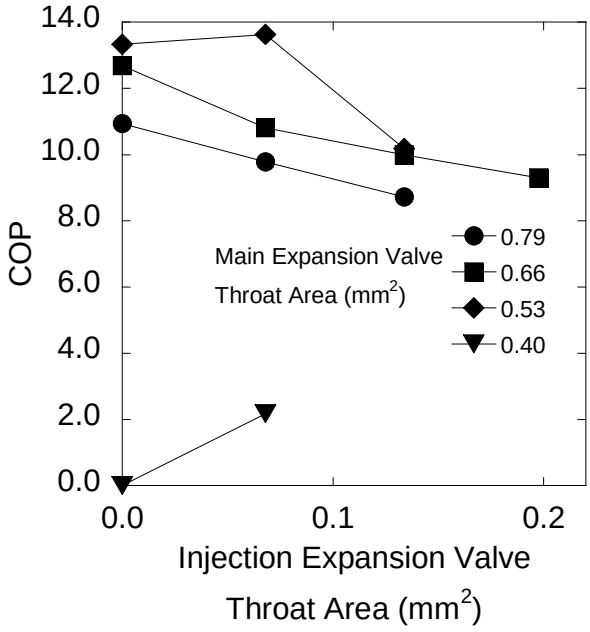

Fig. 2.10 COP with respect to change of injection expansion valve opening (m_{charge}: 1100 g)

obtained heat from compression work is more dominant than the absorbed heat at evaporator extra, COP becomes to decrease. Fig. 2.10 shows these cases.

In Fig. 2.11, pressure-enthalpy diagram of vapor injection cycle is presented when main expansion valve throat area is 0.40 mm^2. When the main expansion valve opening is too small, condenser pressure upraises and excessive compression work is consumed. In that case, refrigerant fed from compressor to condenser becomes small because of the increased pressure resistance of the main expansion valve. If vapor injection is applied to the system, the refrigerant enthalpy at expansion valve inlet becomes to smaller because of heat rejection at internal heat exchanger and flow resistance at the main expansion valve can be decreased significantly while similar amount of mass flow rate circulates through main expansion valve. Because injected refrigerant flows out through the injection expansion valve, the reduced flow resistance makes more refrigerant to goes out from condenser than the fed refrigerant and finally the condenser pressure takes the lowered pressure to balance fed refrigerant and leaving refrigerant. In this case, the excessively high condenser pressure becomes lowered and COP increases.

However, if refrigerant which flows in condenser becomes too much compared to condenser size and condensing pressure is not sufficiently high,

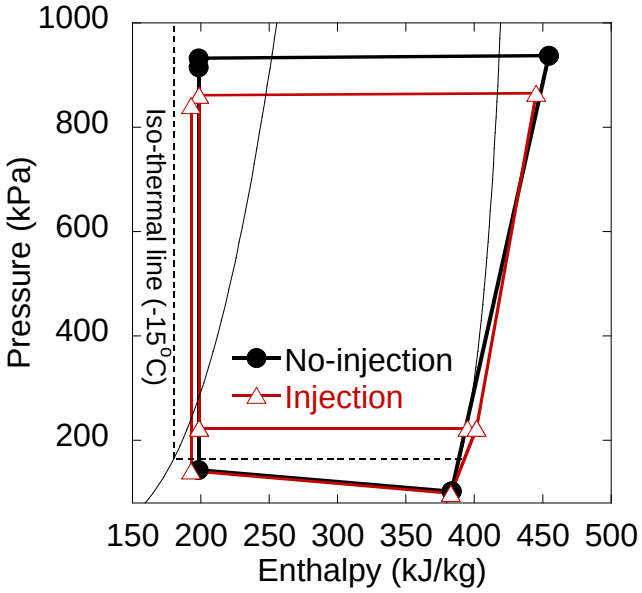

Fig. 2.11 Pressure-enthalpy diagram of no-injection heat pump and injection applied heat pump ($A_{throat,\ main}$: 0.40 mm^2, $A_{throat,\ inj}$: 0.07 mm^2, m_{charge}: 1100 g)

heat transfer performance of condenser deteriorate. This induces higher refrigerant enthalpy at condenser outlet and the refrigerant enthalpy at the main expansion valve inlet might increase although internal heat exchanger exists. This situation induces net refrigerant flow at condenser positive and the condenser pressure becomes upraised. The upraised condenser pressure encourages heat transfer at condenser and increases mass flow rate at expansion valve and final balanced condenser pressure can be determined. It is presented in Fig. 2.9 and because there is no COP improving factor but COP decreasing factor exists, COP becomes lowered.

As a summary, there are two contradictive factors one of which makes condenser pressure increased and the other decreased. If condenser pressure is sufficiently high and mass flow rate does not exceed the appropriate amount, applying vapor injection lowers condenser pressure and if not, the condenser pressure moves vice versa. This also influences COP and if effect of pressure decrement is dominant, COP increases and vice versa.

In the aspect of main expansion valve opening, Fig. 2.10 shows there exists optimal main expansion valve opening. Too large expansion valve opening causes low condenser pressure and low heat transfer efficiency at condenser while too small expansion valve opening causes excessively high condenser pressure and much compression work. This characteristics show

that it requires optimum COP control but one should note that the most important requirement is heat capacity.

Fig. 2.12 shows heating capacity with respect to change of refrigerant mass charge. Heating capacity generally increases as more refrigerant is charged into the system. Large refrigerant charge helps condenser pressure to be upraised and enhances heat transfer at condenser. More heat rejection at condenser generally decreases enthalpy at evaporator outlet enhancing heat absorption in evaporator. It should be noted that heating capacity generally shows increasing trend with respect to increase of injection expansion valve opening at most of the refrigerant charge amount. However, in Fig. 2.12 (c) which shows the case when main expansion valve opening is too small, injection makes heating capacity decreased when refrigerant mass charges are 900 and 1000 g. In those cases, very small main expansion valve opening causes DSH at compressor suction and density of refrigerant becomes decreased resulting in small mass flow rate. In this situation, by applying vapor injection technique makes internal heat exchanger flood and it causes effect of decreasing of refrigerant mass charge with lower evaporation pressure. It induces lower refrigerant density at compressor suction again and heating capacity is reduced. However, if refrigerant mass charge is sufficient, extra liquid refrigerant at accumulator buffers the refrigerant mass

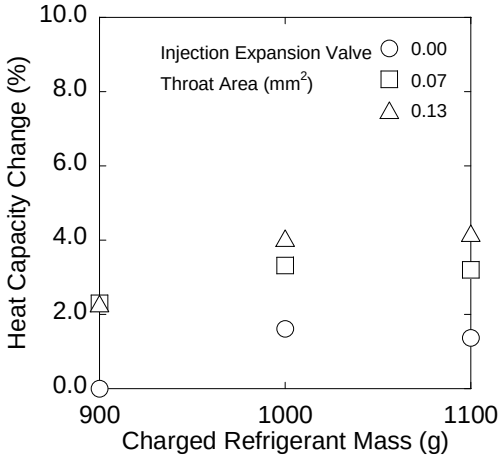

(a) Main Expansion Valve Throat Area: 0.79 mm^2

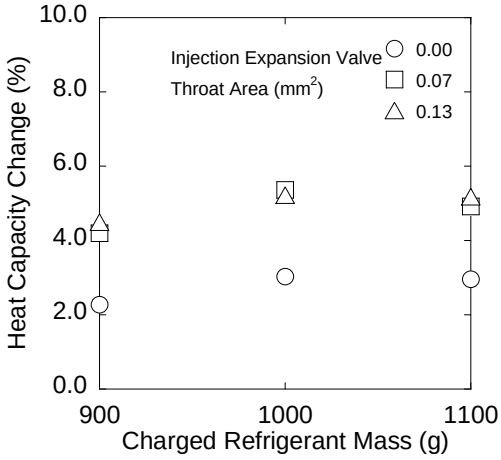

(b) Main Expansion Valve Throat Area: 0.66 mm^2

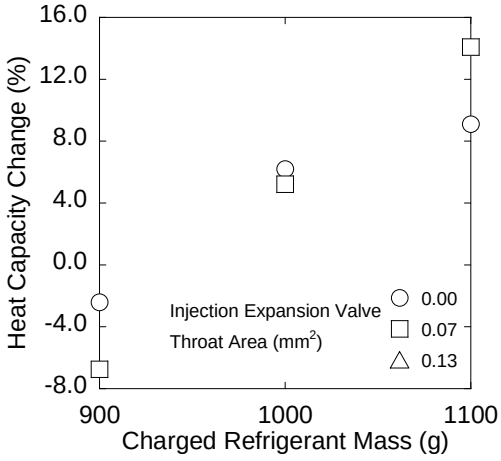

(c) Main Expansion Valve Throat Area: 0.40 mm^2

Fig. 2.12 Heat capacity change with respect to refrigerant mass charge

charge decreasing effect caused by vapor injection and vapor injection makes heat capacity increased.

2.4.2 Analysis on the Steady State Response of the System

In the previous section, the system behavior with regard to vapor injection technique was investigated. This section will treat the other detailed system state change caused by vapor injection.

In Fig. 2.13, change of pressure at the internal heat exchanger low pressure side outlet is presented. This represents injection pressure at which refrigerant is pushed into injection hole and compressor chamber. Because there exists pressure resistance at injection hole, the injection pressure is one of important factors for determining injection mass flow rate. In the figure, the injection pressure upraises as injection expansion valve opening increases. This upraised injection pressure enhances injection flow at injection hole and mass flow rate passing thought condenser also increases. By comparing Fig. 2.13 with Fig. 2.6, it is found that the increase of mass flow rate is closely related with injection pressure. The flow rate of injected refrigerant directly increases heating capacity and this effect is presented in Fig. 2.5. However, in the aspect of heat transfer at internal heat exchanger

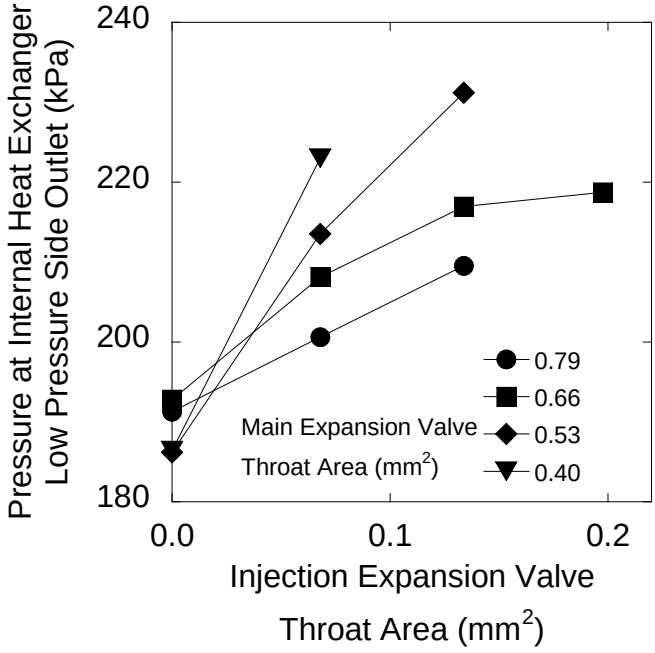

Fig. 2.13 Change of injection pressure with respect to injection expansion valve opening change (m_{charge}: 1100 g)

and DSH at internal heat exchanger low pressure side outlet, upraise of injection pressure is not just good. The upraised injection pressure induces higher evaporating temperature of refrigerant at internal heat exchanger low pressure side inlet and it deteriorates heat transfer at the internal heat exchanger. As increasing opening of injection expansion valve, heat transfer in internal heat exchanger decreases while injected refrigerant mass flow rate increases, DSH at internal heat exchanger low pressure side outlet becomes lowered. Fig. 2.14 shows this trend.

The refrigerant temperature at compressor discharge is one of the important factors when considering heating solution in cold region. If evaporator temperature is very low, isentropic compression work is increased and compressor discharge temperature goes up excessively. The excessive temperature of refrigerant might make quality of lubricant oil degrade and necessarily avoided. Referring to Fig. 2.15, it can be told that when the refrigerant temperature at compressor discharge port is excessively high, it seems to be lowered by applying vapor injection technique with higher heat capacity. This is the case when main expansion valve opening is too small. On the contrary, when the refrigerant temperature at compressor outlet is too low, heat transfer at condenser is decreased and the system performance becomes poorer. For such a case, by applying vapor injection

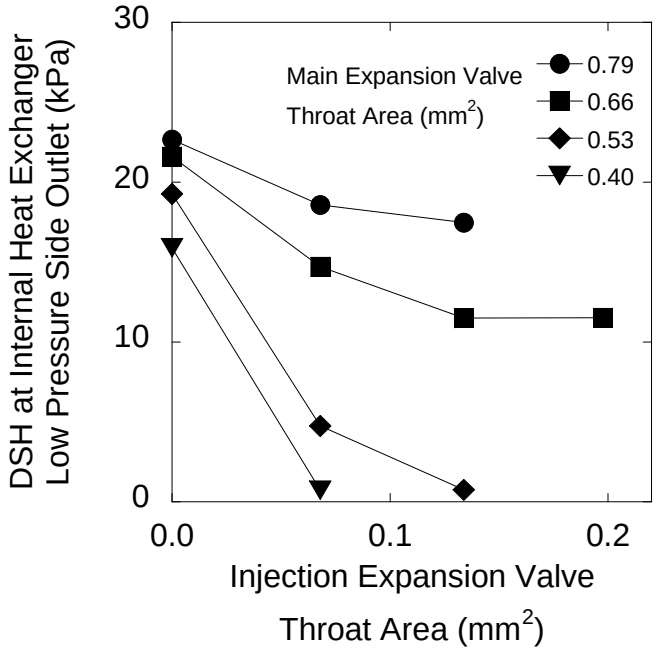

Fig. 2.14 Change of DSH at internal heat exchanger low pressure side outlet with respect to injection expansion valve opening change (m_{charge}: 1100 g)

technique, one can upraise the compressor discharge temperature and it is also presented in Fig. 2.15.

Fig. 2.16 shows change of DSC at condenser outlet when main expansion valve opening and injection expansion valve opening varies. DSC is large when main expansion valve opening is small and small when main expansion valve opening is large. It also decreases as injection expansion valve opening increases. Additionally to this general trend, it is notable that all the DSC values are larger than 10 K which is fairly large. This is because of the small condenser size compared to evaporator size. The temperature difference between evaporating temperature and secondary fluid inlet temperate at evaporator is less than 4 K while the temperature difference between condensing temperature and secondary fluid temperature is about 35 K with 50 K maximum. If the temperature difference between condensing temperature and secondary fluid temperature is small, DSC becomes decreased and COP might be higher but heating capacity becomes insufficient. In this reason, condensing temperature should be maintained at comparatively high temperature and DSC at condenser outlet becomes large.

This large DSC affects badly on vapor injection. If DSC is large, this means low enthalpy at condenser outlet because enthalpy of saturated liquid does not vary although condensing pressure changes. Hence maximum

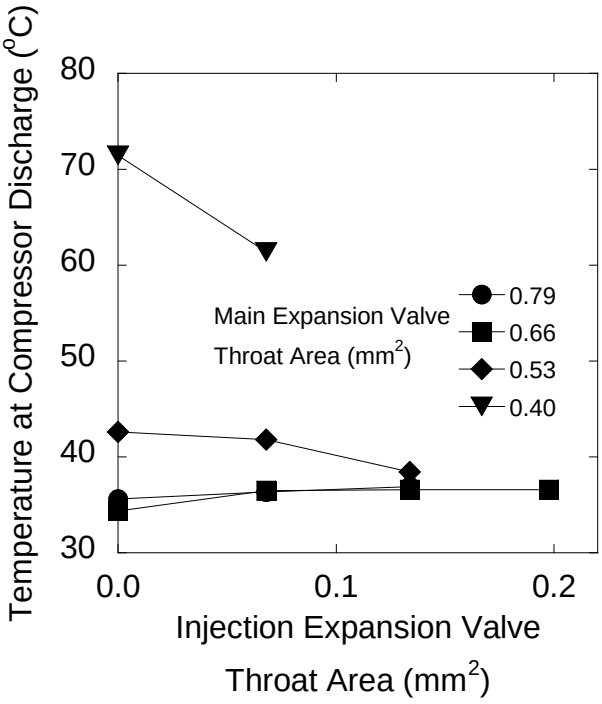

Fig. 2.15 Compressor discharge temperature change with respect to change of injection expansion valve opening (m_{charge}: 1100 g)

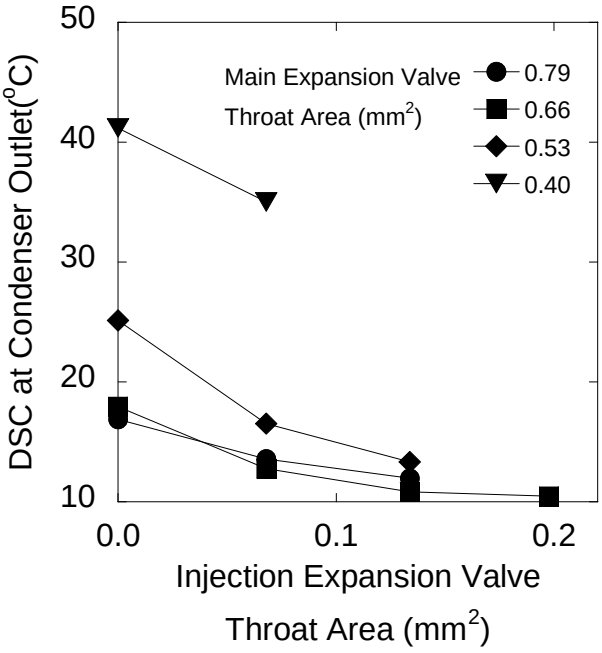

Fig. 2.16 Change of DSC at condenser outlet with respect to change of injection expansion valve opening (m_{charge}: 1100 g)

capable heat transferred at internal heat exchanger becomes decrease and DSH at internal heat exchanger low pressure side outlet falls to zero rapidly in Fig. 2.14. Large DSC also generally represents low temperature and makes heat transfer at internal heat exchanger worse. Fig. 2.17 shows temperature at condenser outlet.

Pressure of evaporator is one of the interesting characteristics which affect system performance. Change of the pressure at evaporator inlet is presented in Fig. 2.18. When main expansion valve opening is large, the pressure at evaporator inlet increases at first as injection expansion valve opening increases. When main expansion valve opening is large, condenser pressure is upraised as injection is performed and this leads more refrigerant feeding to evaporator. Hence evaporating pressure and compressor suction pressure elevate. After that, more injection causes lower enthalpy at evaporator inlet and more flooding in evaporator. This makes evaporator pressure decreased. On the other hand, if main expansion valve opening is small, condenser pressure does not increase and evaporator inlet enthalpy decreases. More flooding occurs in evaporator and evaporator pressure becomes decreased.

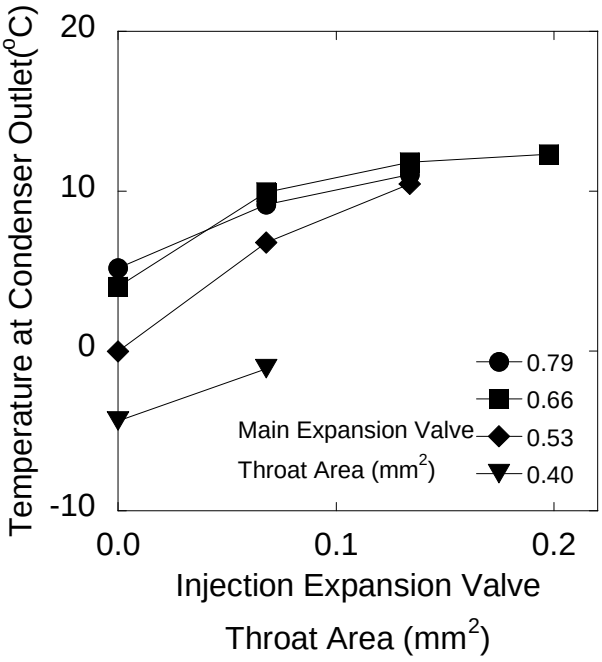

Fig. 2.17 Change of temperature at condenser outlet with respect to change of injection expansion valve opening (m_{charge}: 1100 g)

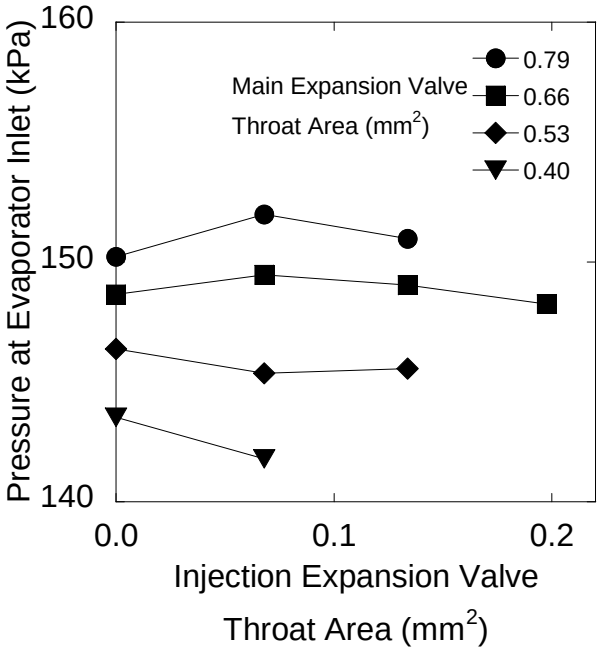

Fig. 2.18 Change of pressure at evaporator inlet with respect to change of injection expansion valve opening

2.5 Conclusion

A heat pump system using R134a as refrigerant was investigated for application of vehicle heating solution. Vapor injection technique was adopted to increase heating capacity and its steady state characteristics were analyzed qualitatively. The heat pump system used for vehicle contains an evaporator of sufficient scale and comparatively small condenser. Additionally, it requires the largest heating capacity under start-up conditions when indoor temperature and outdoor temperature are the same. In this study, -15˚C was set for both condenser and evaporator secondary fluid to simulate the start-up conditions experimentally in wind tunnel. Characteristics of vapor injection heat pump system with respect to refrigerant charge, main expansion valve opening and injection expansion valve opening were obtained by experiment.

By the experimental results, it can be concluded that as increases vapor injection amount, heating capacity also increases with small decrease of COP. Hence vapor injection technique can be regarded as a good solution for a vehicle heat pump. However, refrigerant charge also takes significant role in determining heating capacity. By selecting large refrigerant charge amount, heating capacity was increased fairly while COP was degraded much. Use of vapor injection into the system its heat capacity increased more and

degradation of COP was reduced. In this reason, one can conclude that the controlling of condenser pressure by adjusting main expansion valve and refrigerant charge amount is very important for using vapor injection technique. The more general investigations will be presented in the following chapter by numerically.

Chapter 3. Analytical Investigation on the Performance Improvement of a Heat Pump Using Vapor Injection Technique

3.1 Introduction

In the previous chapter, steady state characteristics of vapor injection heat pump system were studied. In the study, it was shown that the steady state characteristics of vapor injection system which applied to relatively small condenser and the same indoor and outdoor temperature conditions are slightly different. In this chapter, the characteristics of vapor injection heat pump will be analytically investigated. The reason of steady state behavior of vapor injection heat pump with respect to change of operating conditions will be explained.

At first, one of the most important characteristics of vapor injection system which is applied to the mobile heat pump environment is that the effect of an internal heat exchanger is less significant for increasing heat capacity. Fig. 3.1 shows pressure-enthalpy diagram for a heat pump system when DSC at condenser is large. For both cycles, it is assumed that evaporator

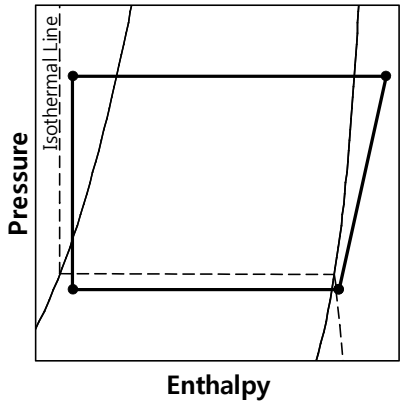

(a) Normal cycle

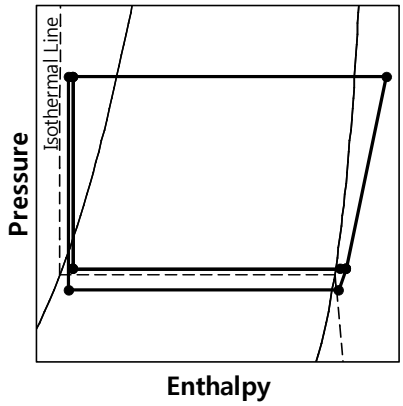

(b) Vapor injection cycle

Fig. 3.1 Pressure-enthalpy diagram for comparison between normal cycle and vapor injection cycle when DSC at condenser is large

is relatively large compared to condenser and the dashed isothermal line represents the same indoor and outdoor temperature. The condenser pressure is 1000 kPa, evaporator pressure is 400 kPa and vapor injection pressure is 460 kPa. DSC was set to 21˚C and isothermal line represents 12˚C. It should be noted that at compressor suction, the same amount of refrigerant is taken in if the swept volume of compressor is fixed and density and pressure at compressor suction is constant. In this reason, considering Eq. 3.1, the augment of heating capacity by applying vapor injection is determined enthalpy decrement at evaporator inlet and increased compressor work.

$$\dot{Q}_{heat} = \dot{Q}_{cool} + \dot{W} = \dot{m}_{evap}(h_{evap,out} - h_{evap,in}) + \dot{W} \tag{3.1}$$

The refrigerant state at evaporator outlet is assumed saturated vapor and evaporation pressure generally varies small because evaporator is relatively large. In this state, when comparing Fig. 3.1 (a) and (b), the refrigerant enthalpy at evaporator inlet decreases very small amount by applying vapor injection. Hence it can be concluded that increase of heating capacity caused by vapor injection is very small amount when it is compared with normal cycle which has large DSC.

However, as stated in the previous chapter, the increment of work also provides additional heating capacity in vapor injection heat pump system and one should observe the increased mass flow rate passing through condenser to

comprehend the performance enhancement of vapor injection system. If one tries to inject only 'vapor' refrigerant, the amount of refrigerant which can be injected is very tightly limited by the heat transfer amount in internal heat exchanger. If the heat in internal heat exchanger which the injection refrigerant can obtain is very small, its mass flow rate should be decreased. In Eq. 3.2, the enthalpies at internal heat exchanger low pressure side inlet and outlet can be regarded as constant and the mass flow rate is directly proportional to the transferred heat.

$$\dot{Q}_{IHX} = \dot{m}_{inj}(h_{IHX,low,in} - h_{sat.vap,P_{IHX,low,out}}) = UA_{IHX}\Delta T_{IHX} \quad (3.2)$$

In this reason, the increment of heating capacity caused by the increment of work also does not expected to increase significantly. To comprehend the performance increment of vapor injection more exactly and to construct the design and control strategy of a vapor injection heat pump system for electric vehicle, it is required to simulate a vapor injection compressor and analyze the system performance using more detailed numerical model. The task of the investigation also contains to find out the potential of performance enhancement of vapor injection heat pump system.

3.2 Modeling of Vapor Injection Heat Pump System

In general, the vapor injection technique is applied to vapor compression

system which uses scroll compressor. Recently, scroll compressor is actively adopted in heat pump system owing to the development of manufacturing technology. Scroll compressor also provides good environment to perform vapor injection. For a scroll compressor, vapor injection hole can be easily manufactured and it can be opened and closed at appropriate time without any timing control method.

In this study, simulation of a scroll compressor is mainly consists of describing the state of suction and compression chamber and calculate calculating mass flow rate of refrigerant by suction and injection. Work consumed by compressor is also one of the considerations.

In a scroll compressor refrigerant is compressed in chamber which is formed by two involute curved wraps. One of which rotates and squeezes chamber and the other is fixed. Fig. 3.2 shows conceptual cross sectional view of a vapor injection scroll compressor. The lighter scroll wrap represents rotating scroll and the darker scroll wrap represents fixed scroll wrap. When the rotating scroll wrap blocks the two holes which places at the case of the scroll compressor, vapor injection does not occur while the vapor injection is performed when the hole is opened. Using to this characteristic, vapor injection can be performed at appropriate mid-pressure.

At neat the center region of scroll compressor, some special curve which

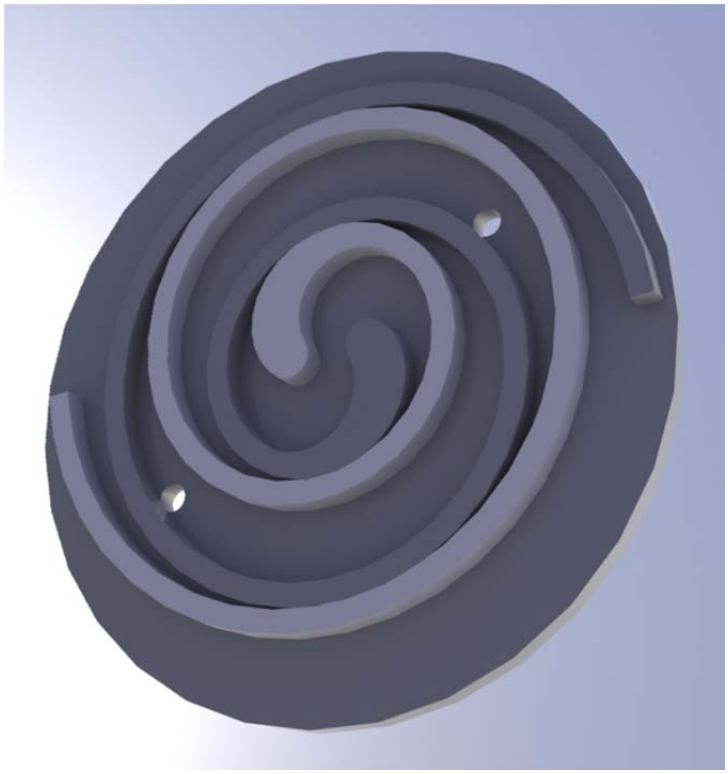

Fig. 3.2 Conceptual cross sectional view of a vapor injection scroll compressor

makes the compression motion smooth and complete is required. It is called perfect mash profile (PMP) and PMP suggested by Liu *et al*. (1992) was used in simulating scroll compressor in this study. Profile of scroll wrap is generally circle of involute and it can be presented by mathematical expression such as Eq. 3.3 with parametric equations.

$$r = a\sqrt{1 + (t - t_0)^2} \qquad (3.3\ (a))$$

$$\theta = t - \arctan(t - t_p) \qquad (3.3(b))$$

The volume of chamber surrounded by two scroll wraps is calculated by referring to Kim (1998). Injection holes are bored at 180˚ before the involute ending angle. Most of the geometrical factors are determined similarly to the compressor which was used in experimental investigation. Table 3.1 shows the used parameters for modeling of scroll compressor and Fig. 3.3 shows the real profile of two scroll wrap. Each axes represents length by metric dimension. The solid line is fixed scroll and dashed line represents rotating scroll.

The opened area of injection hole with respect to rotating of rotating scroll is calculated by referring Liu *et al*. (2009). It assumes the profile scroll wrap which covers injection hole as straight line and by obtaining the shortest distance between the center of injection hole and scroll wrap profile, finds out

Table 3.1 Simulation conditions

Parameters	Value
Compressor RPM	4500
Involute ending angle (°)	About 1000
Base circle radius (mm)	About 3.0
Wrap thickness (mm)	About 5.0
Wrap height (mm)	About 20.0
Beta (°)	16.0
Gamma (°)	94.3
Suction chamber volume (cc)	About 40.0
Vapor injection hole angle (°)	180
Vapor injection hole radius (mm)	1.25, 1.75
Suction pressure (kPa)	100
Discharge pressure (kPa)	600, 800, 1000, 1200

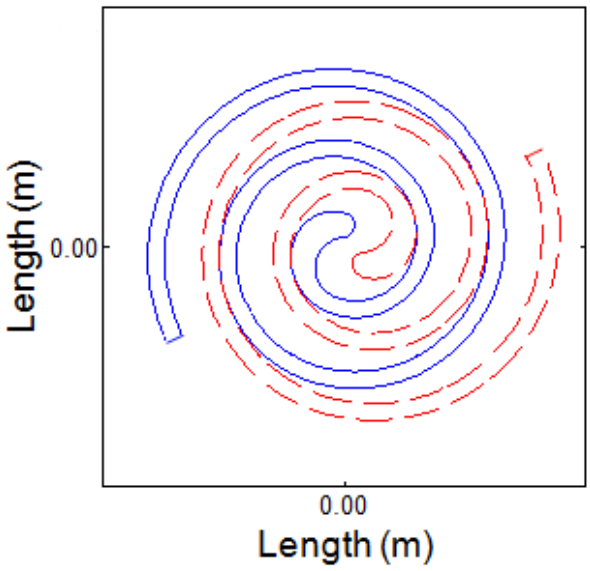

Fig. 3.3 Pressure-enthalpy diagram of phase separator vapor injection cycle when DSC is small and large

the covered and opened area.

3.3 Simulation Results and Discussion

The purpose of this investigation is to find out that at what pressure condenser pressure should be adjusted and injection pressure with given condenser of small size and vapor injection compressor. At first, it is shown that how heating capacity changes as varying injection expansion valve opening. The varying of injection expansion valve opening is reflected into the change of injection pressure. As injection pressure increases, basically the drive force between injection hole inlet and outlet becomes to larger and injection mass flow rate increases. If the flow is choked at injection hole, only the upstream pressure is considered and it also causes larger injection mass flow rate. Hence, as presented in Fig. 3.4, heating capacity increases. The limitation of increasing injection pressure is bounded to make the injected refrigerant saturated vapor when IHX effectiveness is 98%.

In the aspect of condenser pressure, as condenser pressure increases heating capacity generally increases but beyond 1000 kPa, the increment becomes very small. The temperature difference between refrigerant and secondary fluid generally increases as condenser pressure is upraised and it enhances heat transfer at condenser. However, with the upraised condenser

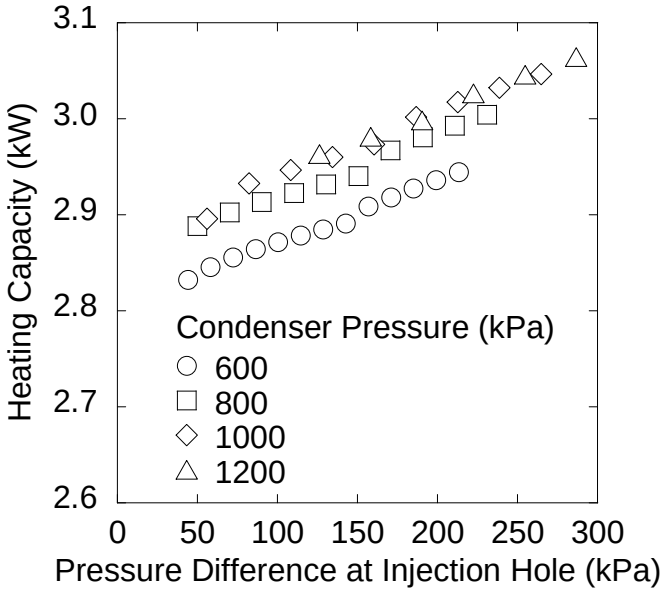

Fig. 3.4 Heating capacity change with respect to injection pressure

pressure, compressor discharge refrigerant which enters into the condenser becomes to have much DSH and more portion of condenser is occupied with super heated vapor refrigerant. This makes condenser heat transfer performance degrade. The limitation of the increment of heating capacity caused by upraise of condenser pressure can be explained with the such phenomenon.

Fig. 3.5 shows injection mass flow rate and it is increased as pressure difference between injection hole inside and outside as stated before. However, maximum transferable heat at internal heat exchanger high pressure side decreases as pressure difference at injection hole increases. This trend gives bad effect to obtain heat to vaporize the injected refrigerant. As injection mass flow rate increases more heat is required to vaporize the injected refrigerant but the upraised injection pressure results in higher evaporation temperature of injected refrigerant and it reduces maximum transferable heat at IHX high pressure side. It is certain that liquid injection also increases heating capacity by increasing work consumed at compressor but it should be avoided in general case.

The heat absorbed by the injected refrigerant directly decreases enthalpy at evaporator inlet and according to the first law of thermodynamics, it directly increases heating capacity. However, at large transferable heat

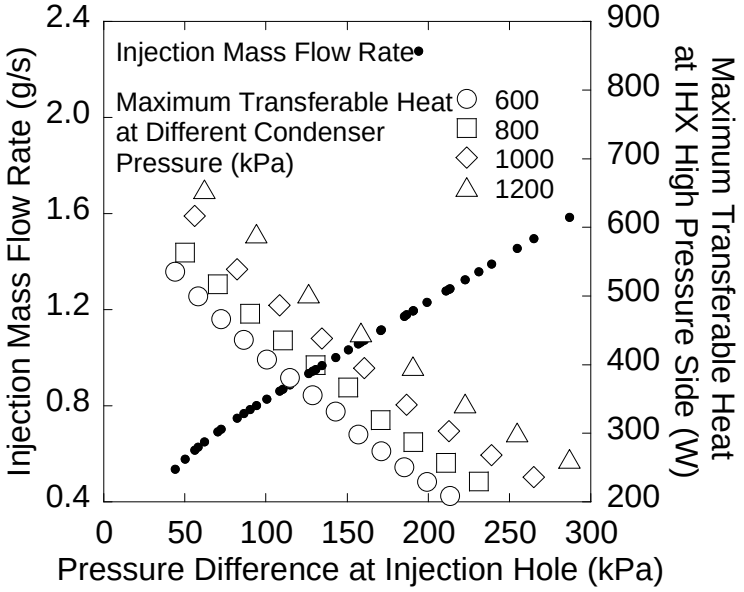

Fig. 3.5 Change of injection mass flow rate and the maximum possible heat transfer at IHX high pressure side with respect to change of pressure difference between injection hole inlet and outlet (P_{suc}: 100 kPa)

condition, injection mass flow rate is too small and the maximum transferable heat at IHX low pressure side is bound in small value. Hence the heating capacity in Fig. 3.4 with small pressure difference at injection hole shows small increment of heating capacity although maximum transferable heat at IHX high pressure side is large. As a result, at the balanced point between the required heat to vaporize injected refrigerant and the maximum transferable heat, the maximum heating capacity is obtained.

Considering this, to use vapor injection technique more efficiently, to increase injection mass transfer is very important. With larger injection hole diameter, it is expected that one can obtain more injection mass flow rate at the same pressure difference at injection hole. Fig. 3.5 shows heating capacity change with respect to injection pressure when the radius of injection hole is increased from 1.25 mm to 1.75 mm. The figure shows heating capacity is increased more than that of 1.25 mm case.

Moreover, considering COP, Fig. 3.7 shows that the COP of case of 1.25 mm and 1.75 mm does not decrease while heating capacity is increased. In this figure, some characteristics should be pointed out. At first, according to injection mass flow rate increases, COP does not vary much while heating capacity increases. This is different with the real vapor injection system because condenser pressure is constant in this simulation. The purpose of this

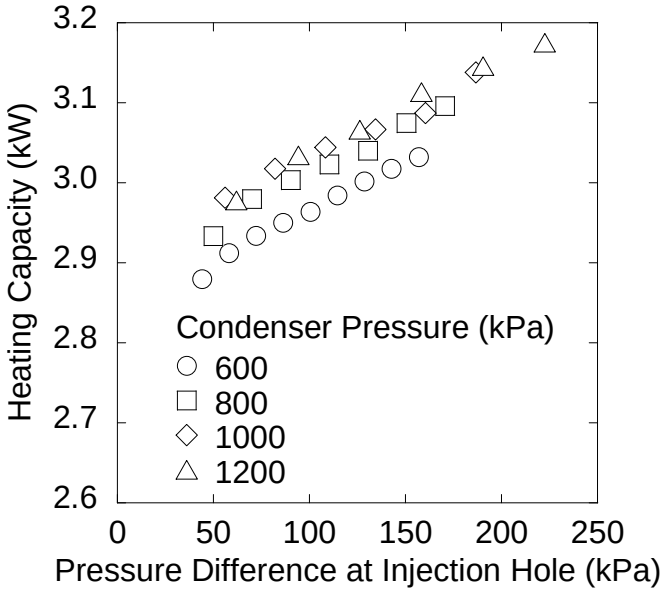

Fig. 3.6 Heating capacity change with respect to injection pressure (r_{inj}: 1.75 mm)

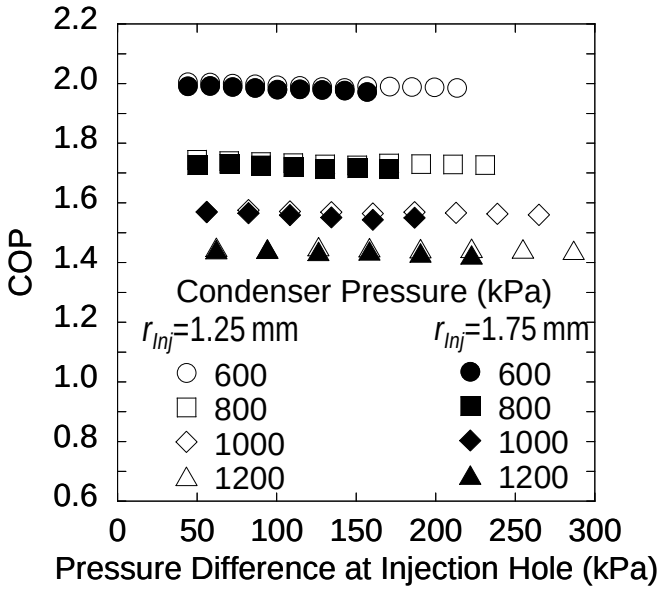

Fig. 3.7 COP change with respect to injection pressure (r_{inj}: 1.25 mm)

simulation is to find out the way of design or control method for a vapor injection system and the problem that how condenser pressure should be controlled is one of the important problems. In a real system, condenser pressure can be controlled by expansion valve opening with appropriate refrigerant charge amount and this simulation will provide useful information for establishing control strategy. Hence it looks like there exists some different behavior with a real vapor injection system but by considering related constraints, the simulation can be told that it reflect a real vapor injection system well in some necessary way.

Anyway, the small change of COP with respect to increase of injection mass flow rate means the ratio of the increment of heating capacity to the increment of work is the same with COP. The increase of mass flow rate passing through condenser makes the temperature of one phase state refrigerant decreased more slowly and two phase state maintained longer. In this reason overall ΔT between refrigerant and secondary fluid becomes larger and heat transfer increase. Moreover, more mass flow rate also increases heat transfer coefficient at refrigerant side and $UA\Delta T$ becomes larger. If $UA\Delta T$ does not vary, heating capacity will not increase and condenser outlet enthalpy will be decreased. However, if the rate of increase of $UA\Delta T$ is matched with that of mass flow rate, condenser outlet enthalpy does not vary much. Also,

throttling effect at injection hole makes increased enthalpy at compressor discharge and enthalpy difference between condenser inlet and outlet varies in small amount (Fig. 3.8). The final increase of increased mass flow rate combined with the enthalpy difference change but the effect of mass flow rate change is more dominant. Under this situation, injection hole places near the suction region and because of throttling effect, the injected refrigerant compresses from near suction pressure to discharge pressure. Hence, the final situation is that increase of mass flow rate with the same pressure-enthalpy diagram. To obtain efficiency increment, it is required to increase injection hole angle.

3.4 Conclusion

In this chapter, vapor injection technique was investigated numerically. The effect of vapor injection technique for a heat pump was not comprehended yet while it has been widely used in many. This study can provide useful information on controlling and designing a vapor injection heat pump. Especially a heat pump system is selected as an object system and its special properties such as comparatively small condenser and the same low temperature condition for indoor and outdoor were considered.

For control strategy, it was shown that it is good to upraise condenser

pressure to a certain level for increasing heat capacity but beyond some certain value, effect of condenser pressure upraise was significantly degraded while COP continuously decreases. In this reason, determining optimal condenser pressure is one of the important tasks of controlling vapor injection heat pump.

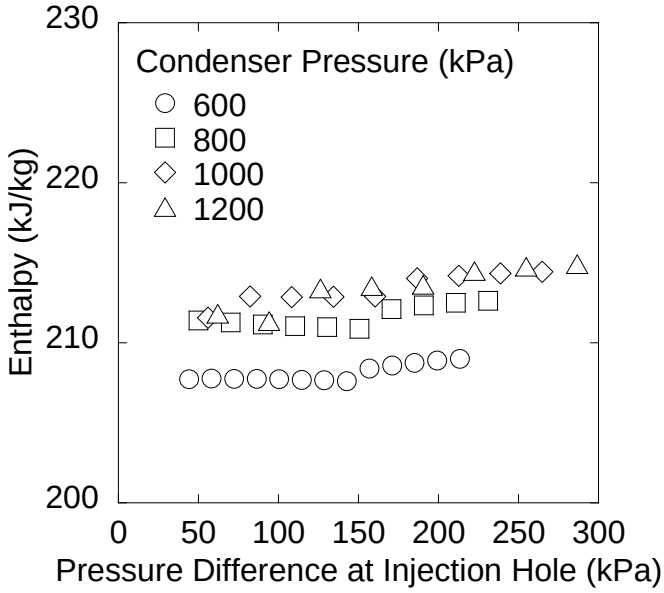

Fig. 3.8 Change of enthalpy at condenser outlet with respect to pressure difference at injection hole (r_{inj}: 1.25 mm)

Chapter 4. Real Time Optimal Control Method of Heat Rejection Pressure for CO_2 Refrigeration System

4.1 Introduction

CO_2, one of the most popular natural refrigerants has no ozone depletion effect and very low global warming effect but its low critical temperature causes a complicated control problem. A general refrigerant system shows the highest energy efficiency when its DSH (degree of super heat) and DSC (degree of super cool) are small value. However, in a CO_2 refrigeration system, it is impossible to determine DSC in heat rejection process because heat rejection process of a CO_2 refrigeration system occurs in super-critical state in general. During this super-critical heat rejection process, gas like CO_2 which a compressor discharges changes to dense liquid like state as heat is rejected. The heat exchanger which is used for heat rejection process in a CO_2 refrigeration system is so called gas-cooler and there exists no DSC concept. Fig. 4.1 shows typical temperature-entropy diagram of two refrigerant cycles which use CO_2 and R134a as refrigerant

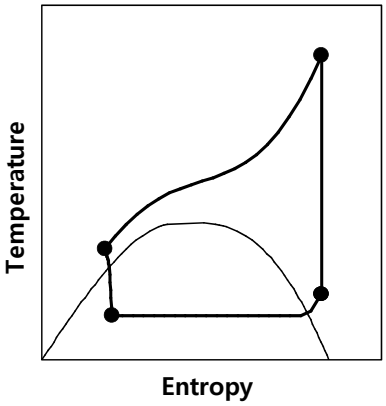

(a) CO_2

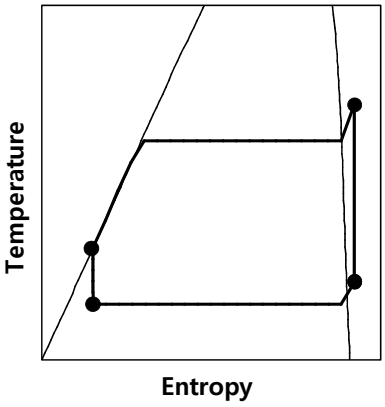

(b) R134a

Fig. 4.1 Temperature-entropy diagram of typical refrigeration cycle which use refrigerant CO_2 and R134a

for each case.

As shown in the figure, CO_2 refrigeration cycle shows no DSC during heat rejection process and moreover, increment of entropy during throttling process should be concerned. In this reason, an internal heat exchanger is generally used for a CO_2 refrigeration system. Using internal heat exchanger, one can obtain extra heat or cooling capacity resulting in higher COP. However, with an internal heat exchanger, the refrigerant quality at evaporator outlet can be less than 1 and one cannot determine optimal expansion valve opening using DSH at evaporator outlet. Fig. 4.2 shows schematic of CO_2 refrigeration system with an internal heat exchanger.

Hence, for a CO_2 refrigeration system, DSC and DSH cannot be used as designate for controlling expansion valve opening. In general refrigeration system there are two values which should be controlled. One is the efficiency as stated above and the other is cooling or heating capacity. The capacity is usually adjusted by changing compressor operating frequency and expansion valve opening is varied to make the system high efficiency. CO_2 refrigeration system also can use compressor operating frequency for capacity control and expansion valve opening for efficiency control but there exists no value which designates high efficiency state such as DSH and DSC. Many of researchers have been studied on this problem and the research

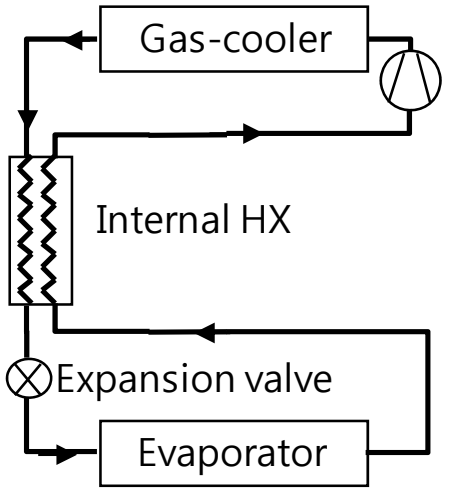

Fig. 4.2 Schematic of CO_2 refrigeration system with an internal heat exchanger

showed that there exists close relationship between heat rejection pressure and COP.

The problem can be explained by referring to Fig. 4.3. Assume that the heat rejection side surrounding temperature is T_1 and the refrigerant temperature at gas-cooler outlet is also T_1. Then, one can consider and compare the performance of two systems whose heat rejection pressures are $P_{gc,low}$ (A, B_l, $C_{1,l}$, $D_{1,l}$) and $P_{gc,high}$ (A, B_h, $C_{1,h}$, $D_{1,h}$), respectively. In this case, the cycle of $P_{gc,low}$ (A, B_l, $C_{1,l}$, $D_{1,l}$) has higher COP than the cycle of $P_{gc,high}$ (A, B_h, $C_{1,h}$, $D_{1,h}$). As the heat rejection pressure changes from $P_{gc,low}$ to $P_{gc,high}$, the specific compressor work increases as $B_h - B_l$ and specific cooling capacity increases $C_{1,l} - C_{1,h}$. If the increment of specific cooling capacity is fairly larger than the increment of specific compression work, the COP of the system of $P_{gc,high}$ becomes higher than that of the system of $P_{gc,low}$. In case of T_{amb1}, the augmented cooling capacity is not larger than augmented compression work enough and COP decreases with the rise of heat rejection pressure. On the contrary, in the case of the heat rejection side ambient temperature and the refrigerant temperature at gas-cooler outlet both being T_2, as the heat rejection pressure changes from $P_{gc,low}$ to $P_{gc,high}$, much more cooling capacity is acquired than the increased compression work. One can expect higher COP when the system forms cycle $P_{gc,high}$ (A, B_h, $C_{1,h}$, $D_{1,h}$).

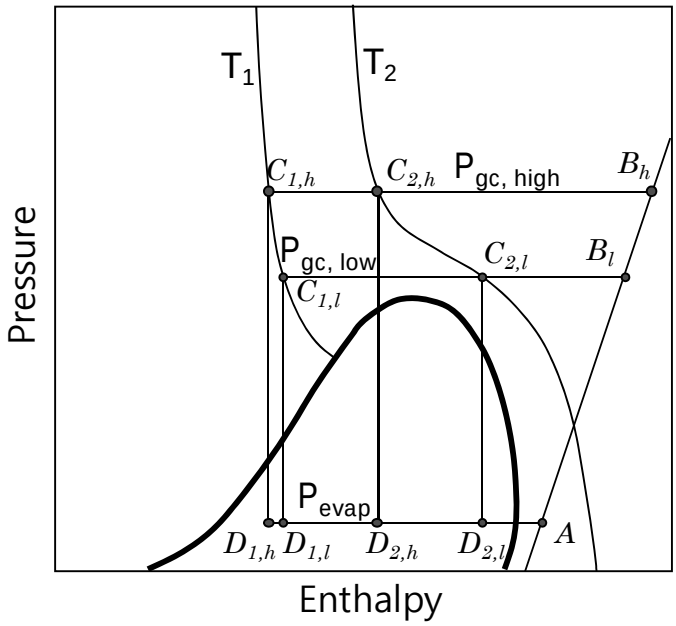

Fig. 4.3 Pressure-enthalpy diagram of CO_2 refrigeration cycle

For both cases, no clear indicating factor which correlates the heat rejection pressure with the system performance (COP) is found and it is a difficult problem to decide heat rejection pressure for the best performance.

In this study, a new efficiency control method which uses expansion valve opening will be suggested relating with heat rejection pressure. Experimental validations and discussion about some limit and improvements are presented.

4.2 Literature Review

The control problem of CO_2 refrigeration system has attracted much of concerns of many researchers and there are many related research studies. Inokuty (1923) suggested a graphical method of finding optimal heat rejection pressure of CO_2 refrigeration system. If temperature of cooling fluid is known and refrigerant state at compressor suction is saturated vapor, the method provides a good approximation of optimal heat rejection pressure. However, it was just a method to calculate the optimal heat rejection pressure under the given system state and did not evolve into a control method.

After the Inokuty's study, especially in recent years, many of the study

were conducted to develop appropriate correlations by which optimal heat rejection pressure can be approximated. Hwang and Radermacher (1998) made simulation programs for CO_2 refrigeration system and R22 refrigeration system with detailed component models. Using the simulation program they calculated the optimum heat rejection pressure with respect to various gas-cooler secondary fluid temperature. Kauf (1999) proposed a formulation for calculating the optimum heat rejection pressure using steady state simulation data. It was the first order polynomial equation with one variable which is temperature of ambient or refrigerant. Liao *et al.* (2000) also proposed a correlation of optimal heat rejection pressure for a CO_2 air-conditioning system based on simulation data. Sarkar *et al.* (2004) conducted a simulation study for a CO_2 heat pump cycle for simultaneous cooling and heating applications. They proposed two correlations which estimate maximum COP of the system and optimum discharge pressure. Chen and Gu (2005) studied the optimum high pressure for CO_2 trans-critical refrigeration systems with different internal heat exchanger efficiencies. They showed that evaporating temperature has little influence on the optimal heat rejection pressure. The effect of the effectiveness of internal heat exchanger on the system performance and on the optimum high pressure was also discussed. Cecchinato *et al.* (2010) reviewed and validated optimal heat rejection

pressure correlations for a CO_2 refrigeration system in various literatures and showed that correlations which adopt gas-cooler outlet temperature as independent variable show better performance than the others. Wang *et al.* (2013) devised dual expansion CO_2 heat pump system with internal heat exchanger. They conducted experimental and analytical studies on the dual expansion CO_2 system and the effect of gas-cooler pressure on the system performance was investigated. It was shown that there are maximum COP and maximum heat capacity with respect to change of gas-cooler pressure. Baek *et al.* (2013) studied the cooling performance of the CO_2 heat pump system varying refrigerant charge amount, EEV opening, compressor frequency and outdoor fan speed at various outdoor temperatures. Based on the obtained experimental data, they showed that there are some specific optimum points under given conditions.

Except the Inokuty's study, these studies proposed correlations which correlate some operating parameters with the optimal heat rejection pressure. However, if the correlations are used for controlling heat rejection pressure of a CO_2 refrigeration system, the applicable operating condition is very limited and the reliability of the control method is highly dependent on the specific system parameters and operating conditions. Moreover, a priori established correlations with much of experimental or simulation data are

required.

To overcome these disadvantages, Zhang and Zhang (2011) devised a correlation free control method of heat rejection pressure for a CO_2 refrigeration system. The idea is simply to compare the COP of a refrigeration system in real time as varying heat rejection pressure and find the value at which the system shows the best COP. However, it seems hard to apply this control method well in a real system because the controller cannot distinct the performance enhancement for transient response and steady state. Cecchinato *et al.* (2012) also proposed a real-time algorithm for the determination of CO_2 refrigeration system using on-line artificial neural network. This method requires complicated neural network algorithm with consistent observation and training process.

4.3 Concept and Implementation of Real Time Optimal Control Method

4.3.1 Concept

To The basic concept of the real time control method introduced is to compare the expected specific cooling capacity increment with the specific work increment. By adopting similar concept of graphical method which is

suggested by Inokuty (1923), the authors developed a real time control method and it was experimentally validated. In this study, the more detailed development process will be introduced and important discussions on the control method would be presented.

The idea of the real time control method starts by considering a very small increment of heat rejection pressure which is generally accomplished by slight close of expansion valve. As heat rejection pressure is upraised, compression work and cooling capacity for specific amount of refrigerant mass flow rate are also increased (Fig. 4.3). In this situation, the ratio of the expected specific cooling capacity increment to the expected specific compression work increment determines whether COP will increase or decrease. The series of equations and inequality (4.1) shows that if the ratio is larger than present COP of the system, COP will increase.

$$\mathrm{COP} = \frac{\dot{Q}}{\dot{W}} \quad \text{and} \quad \mathrm{COP}_{\mathrm{new}} = \frac{\dot{Q} + \Delta\dot{Q}}{\dot{W} + \Delta\dot{W}}$$

$$\text{define} \quad \Delta\dot{Q}_{dum} \equiv \Delta\dot{W}\frac{\dot{Q}}{\dot{W}}$$

$$\text{then} \quad \mathrm{COP}_{\mathrm{new}} = \frac{\dot{Q} + \Delta\dot{Q}_{dum}}{\dot{W} + \Delta\dot{W}} + \frac{\Delta\dot{Q} - \Delta\dot{Q}_{dum}}{\dot{W} + \Delta\dot{W}} = \mathrm{COP} + \frac{\Delta\dot{Q} - \Delta\dot{Q}_{dum}}{\dot{W} + \Delta\dot{W}}$$

$$\therefore \mathrm{COP}_{\mathrm{new}} > \mathrm{COP} \quad \text{when} \quad \left(\frac{\Delta\dot{Q}}{\Delta\dot{W}} > \frac{\dot{Q}}{\dot{W}} \quad \text{or} \quad \Delta\dot{Q} > \Delta\dot{Q}_{dum} \right) \qquad (4.1)$$

To apply the above inequalities, the present COP, expected

‘compression work increment ($\Delta\dot{W}$)’ and ‘cooling capacity increment ($\Delta\dot{Q}$)’ should be calculated based on measured data. Power meter, temperature sensors, pressure sensors and mass flow meters can be used. For practical use, mass flow meters can be replaced by a correlation which correlates fan or compressor operating frequency with mass flow rate of the fluid. If the system is configured by a single loop, ‘compression work increment ($\Delta\dot{W}$)’ and ‘cooling capacity increment ($\Delta\dot{Q}$)’ can be replaced by ‘specific work increment ($\Delta\dot{w}$)’ and ‘specific cooling capacity increment ($\Delta\dot{q}$)’ and in this study, the specific terms are used.

The actual ‘compression work increment’ and ‘cooling capacity increment’ are determined by operating conditions, system specifications and complicated interactions among the components. A simulation program with many iteration loops should be used to estimate the exact behavior of the system and it requires too much calculation processes and time to be used in a real-time control method. For practical use of the control method, appropriate assumptions should be made to let the calculation process be more simple and easy. The assumptions are listed below.

(1) The temperature of the refrigerant at gas-cooler outlet will remain at its present value while the heat rejection pressure rises.

(2) Compression work maintains its present specific compression work

per unit pressure. That is, in Fig. 4.3, the state of refrigerant at compressor discharge port will move along the extension of the line *B*-*C* when small amount of variation is applied to the heat rejection pressure.

(3) The pressure and enthalpy of the refrigerant at compressor suction will remain at its present value while the heat rejection pressure rises.

Assumption (1) is related to the behavior of point *C* in Fig. 4.3. If the present refrigerant state at gas-cooler outlet is $C_{1,l}$, when the heat rejection pressure rises by small amount, it moves along the line T_1.

Assumption (2) determines the variation of shape of line *AB* in Fig. 4.3. If the assumption is applied, the slope of line *AB* will not change when the expansion valve is closed by small amount. In this study, just a simple linear increment of specific compression work was used to see the possibility of application of the suggested control method.

Assumption (3) requires many constraints which conflict with the real behavior of the system. However, these assumptions are necessary to implement the control method and the control performance is fairly acceptable although the assumptions do not reflect real situation.

It should be noted that the assumptions (1) and (2) do not mean that the each value or slope is always constant because the present value is updated in real time reflecting the present operating conditions. These assumptions

consider only the temporary value at present time and if the present value is different from the previous value, it is updated.

With assumption (3), if small amount of heat rejection pressure increment δP is considered, the decrement of refrigerant enthalpy at gas-cooler outlet becomes increment of specific cooling capacity and the ratio can be represented by Eq. (4.2).

$$\left.\frac{\delta \dot{q}_{cool}}{\delta P}\right|_{T_{gc,out}} = \frac{h(P+\delta P, T_{gc,out}) - h(P, T_{gc,out})}{\delta P} \tag{4.2}$$

On the other side, the increment of specific compression work per unit increment of the heat rejection pressure is calculated by Eq. (4.3).

$$\frac{\Delta \dot{w}}{\Delta P} = \frac{h_{comp,dis} - h_{comp,suc}}{P_{comp,dis} - P_{comp,suc}} \tag{4.3}$$

With these equations, the new COP for the increased heat rejection pressure can be written as Eq. (4.4)

$$\mathrm{COP}_{\mathrm{new}} = \frac{\dot{q} + \delta \dot{q}}{\dot{w} + \delta \dot{w}} \approx \frac{\dot{q} + \left.\frac{\partial \dot{q}}{\partial P}\right|_{T_{gc,out}} \delta P}{\dot{w} + \frac{\Delta \dot{w}}{\Delta P} \delta P} \tag{4.4}$$

Additionally, the ratio of increment of cooling capacity to increment of compression work is written in Eq. (4.5).

$$\frac{\delta \dot{q}}{\delta \dot{w}} \equiv \frac{\left.\frac{\partial \dot{q}}{\partial P}\right|_{T_{gc,out}} \delta P}{\frac{\Delta \dot{w}}{\Delta P}\delta P} = \frac{\left.\frac{\partial \dot{q}}{\partial P}\right|_{T_{gc,out}}}{\frac{\Delta \dot{w}}{\Delta P}} \tag{4.5}$$

Finally, as shown in inequality (1), if inequality (4.6) is satisfied, the new COP is higher as heat rejection pressure is increased.

$$\frac{\delta \dot{q}}{\delta \dot{w}} > \mathrm{COP}_{\mathrm{present}} \tag{4.6}$$

Otherwise, if the inequality is not satisfied, one can presume that small decrement of heat rejection pressure will yield much more power consumption saving than decrement of cooling capacity so that COP will be raised with decrement of the heat rejection pressure. This represents how the suggested real time controller operates. In this study, the introduced concept of control method was implemented and its results were analyzed. Moreover, the errors which are caused by the introduced assumptions which do not reflect the real system behavior were discussed.

4.3.2 Implementation

At first, the controller should know several states and values to control the system. Those are (1) the state of refrigerant at gas-cooler outlet, (2) the pressure difference between the compressor suction and discharge, (3) compressor power consumption, and (4) cooling capacity. The cooling

capacity is set by user input because the system can control the capacity by the capacity controller. The capacity controller adjusts compressor frequency to maintain the cooling capacity and it makes the below equation (4.7) valid. A PI controller is used as the capacity controller and it was embodied by LabView program. With the constant capacity controller, if compressor power consumption is known, present COP is easily calculated by dividing the cooling capacity by the power consumption.

$$\dot{Q}_{cool} = \dot{m}(h_{eva,out} - h_{eva,in}) = \text{constant} \tag{4.7}$$

A system schematic which has necessary sensors to obtain the listed information except the cooling capacity is presented in Fig. 4.4. The system has four sensors to implement the control; pressure and a temperature sensor for refrigerant at the gas-cooler outlet, a pressure sensor at compressor suction and a power meter for a compressor. This list of sensors is one of the combinations which can implement the control method with minimum number of sensors to consider economic aspects. For laboratory experiment, however, more sensors were used to obtain more exact information and it is presented in Fig. 4.5.

In any case, refrigerant state at the gas-cooler outlet can be obtained by temperature and pressure information at that point. Enthalpy and isothermal line near the point and $\delta \dot{q}_{cool} / \delta P|_{Tgc,out}$ also can process.

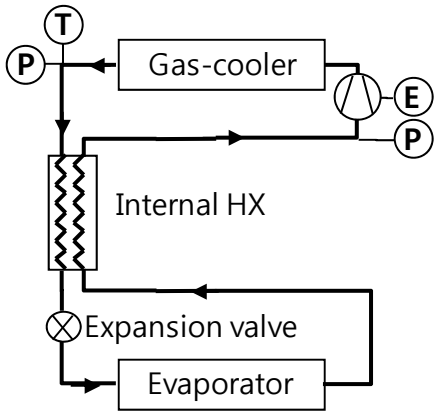

Fig. 4.4 Necessary sensors to implement the real time control method

In any case, refrigerant state at the gas-cooler outlet can be obtained by temperature and pressure information at that point. Enthalpy and isothermal line near the point and $\delta \dot{q}_{cool} / \delta P|_{Tgc,out}$ also can be obtained. In this study, REFPROP 8.0 (Lemmon et al., 2007) is used to calculate enthalpy and isothermal line. $\Delta \dot{w} / \Delta P$ can be calculated with measured pressure values and power consumption. Finally, $\delta \dot{q} / \delta \dot{w}$ (Eq. (4.5)) is obtained dividing $\delta \dot{q}_{cool} / \delta P|_{Tgc,out}$ by $\delta \dot{q}_{cool} / \delta P|_{Tgc,out}$.

Using the above calculations, an electronic expansion valve was controlled to obtain desired heat rejection pressure. The controller was developed as PI controller and embodied by LabView program. By letting the difference between present COP and $\delta \dot{q} / \delta \dot{w}$ be an error term for the PI controller, the expansion valve opening was controlled to be slightly decreased when inequality (6) is satisfied and be slightly increased when it is not.

Additionally, it should be noted that the CO_2 refrigeration system where the control method is applied contains an internal heat exchanger and the internal heat exchanger is a type of liquid line-suction line heat exchanger. Most of the practical CO_2 refrigeration systems are equipped with an internal heat exchanger and it is desirable for considering internal heat exchanger. The assumptions are applied in the very same way as they were firstly

introduced in the previous chapter although an internal heat exchanger was not considered at that time. The obtained results were quite acceptable and the influences of existence of an internal heat exchanger will be discussed in the next chapter.

4.3.3 Experimental Apparatus

The experimental apparatus consists of a CO_2 compressor, an expansion valve, a gas-cooler, an evaporator, an internal heat exchanger and other accessories as presented in Fig. 4.1.

A CO_2 compressor (displacement volume: 12.9 cm^3) and variable frequency inverter was used for controlling cooling capacity. Cooling capacity was calculated by multiplying the enthalpy difference of the secondary fluid by its mass flow rate. The operating frequency was controlled in the range of 40 to 60 Hz for matching required capacity.

A metering valve was used as an expansion valve and a stepping motor system was equipped to control the metering valve. The valve has 0.125 inch of orifice diameter and step motor resolution is 400 pulses per revolution.

Each heat exchanger was a counter type concentric dual tube heat exchanger made by copper. The secondary fluid flowed in the outer tube and the refrigerant flowed in the inner tube for gas-cooler and evaporator. For the

internal heat exchanger, high pressure side was the inner tube. The detailed dimensions and the schematic is presented in Fig. 4.5 and Fig. 4.6. Closed loop system including temperature controllable water bath was used for heat reservoir with water as a secondary fluid. Secondary fluid inlet temperature for each heat exchanger was controlled and set to required constant value.

T-type thermocouple probes were inserted into the tubes and measured refrigerant and secondary fluid temperatures. The uncertainty was estimated about ±0.5˚C. Absolute pressure transducers were installed to measure the high pressure and low pressure. Measurement error was estimated as ±0.15% of full scale value. Differential pressure transducers measured pressure drop in each heat exchanger. Coriolis type mass flow meters measured refrigerant and water mass flow rate. Its reading error was ±0.81%. The compressor power consumption was measured by a power meter and its reading was ±0.3%. Using the uncertainty analysis by Moffat (1988), the uncertainty of cooling capacity and COP were calculated and they are about 5.4% for both values.

4.4 Experimental Results

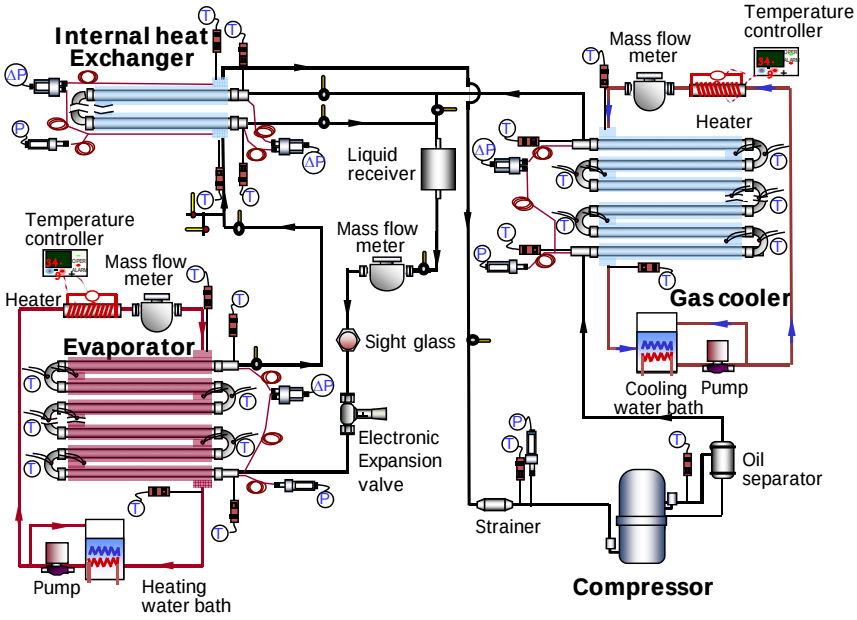

Fig. 4.5 Schematic of experimental apparatus

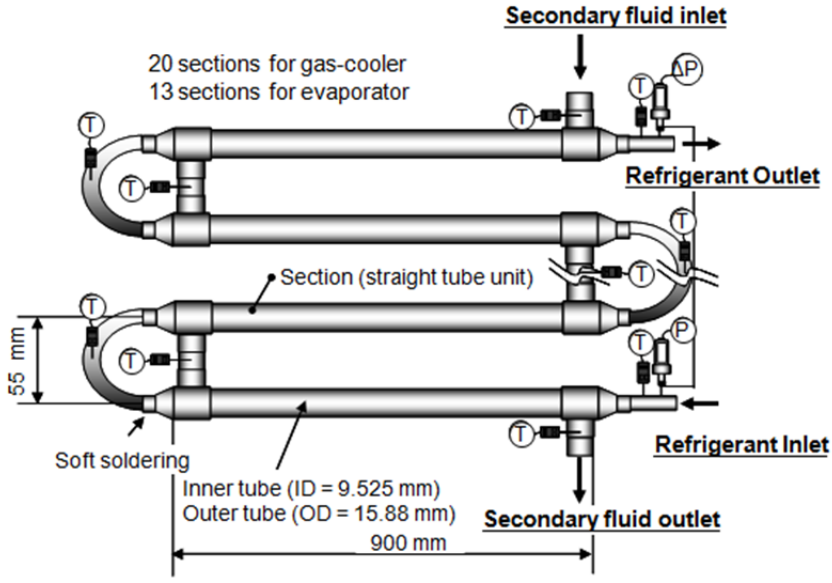

Fig. 4.6 Detailed schematic of the heat exchangers (Lee *et al*., 2014)

First, it will be shown that the proposed real time control method could be applied for controlling heat rejection pressure of a CO_2 refrigeration system and its performance is fairly acceptable. The test apparatus was operated and arbitrary steady state was obtained. Then, after some data acquisition for the steady state, the proposed real time controller started to operate. Expansion valve was changed by the indication of the controller and system responded. The experimental conditions are presented in Table 4.1.

Fig. 4.7 presents behavior of COP, cooling capacity, compressor work and expansion valve opening when the real time control method was applied to a CO2 refrigeration system. The CO_2 refrigeration system was in steady state with fixed expansion valve opening (11.6%) during the first 400 seconds and the real time control process suddenly started at 400 seconds (dashed vertical line). The evaporator secondary fluid inlet temperature was set as 27˚C. In the figure, COP is increased after the controller is turned on and system goes to another steady-state without severely unstable behavior. Fig. 4.7 (b) shows the response of cooling capacity in the same experiment with that of Fig. 4.7 (a). In both figures, the controlled parameters do not diverge or behave unstably. The increase of COP can be explained by ratio of the increments of cooling capacity and compressor power consumption. As stated, the cooling capacity of the system is maintained at constant value 5

Table 4.1 Experimental conditions

Parameter	**Value**
Refrigerant charge (kg)	3
Cooling capacity (kW)	5
Inlet water temperature at gas cooler (˚C)	30
Water flow rate at gas cooler (g/s)	80
Inlet water temperature at evaporator (˚C)	25, 27
Water flow rate at evaporator (g/s)	90
Kp for compressor control	2.4
Ki for compressor control	0.1
Kp for EEV control	0.09
Ki for EEV control	0.005

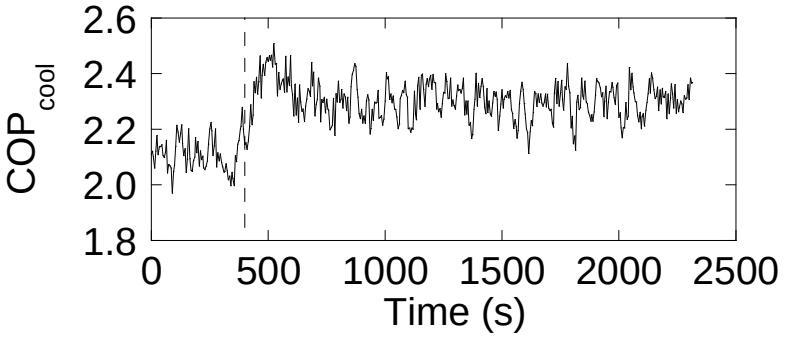

(a)

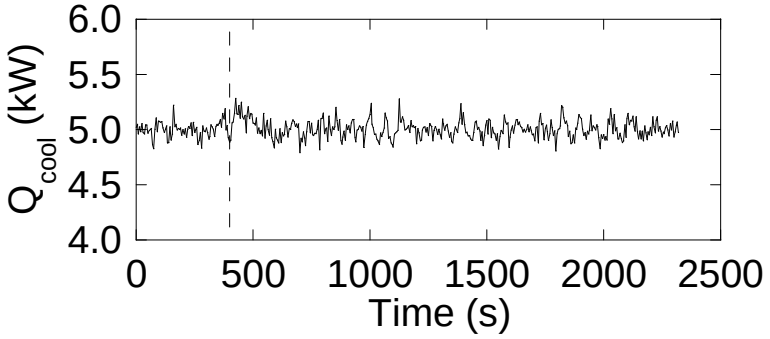

(b)

Fig. 4.7 Response of cooling COP (a), cooling capacity (b), work (c) and expansion valve opening (d) when the real time control starts at specified time ($T_{2nd,\,in}$: 27˚C)

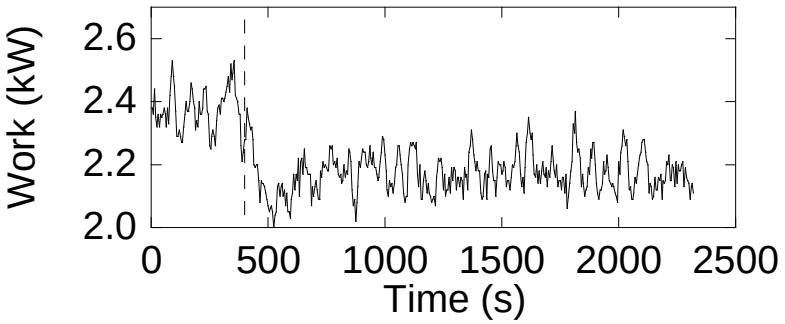

(c)

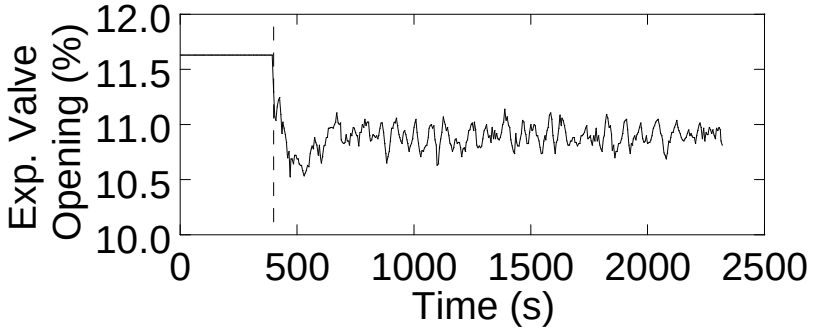

(d)

Fig. 4.7 Response of cooling COP (a), cooling capacity (b), work (c) and expansion valve opening (d) when the real time control starts at specified time ($T_{2nd,\ in}$: 27˚C) (Kim and Kim, 2012) (continued)

kW but 'specific' cooling capacity of refrigerant varies according to change of pressure, temperature and mass flow rate. In the case of Fig. 4.7, the expansion valve opening changes from 11.6% to some controlled value and finally the opening was reduced to about 10.95% (Fig. 4.7 (d)) and gas-cooler pressure was upraised (Fig. 4.8). The specific work becomes larger because of the upraised gas-cooler pressure. However, the increment of specific cooling capacity is more larger and the capacity controller decreases the compressor frequency to reduce refrigerant mass flow rate (Fig. 4.8). As a result, the total compressor work becomes smaller (Fig. 4.7 (c)) and COP becomes larger.

Next the performance characteristics of the real time controller will be presented. Fig. 4.9 displays the steady state COP with respect to different expansion valve opening when cooling capacity is controlled to maintain 5 kW. The expansion valve step was 0.465% of full scale revolution of the expansion valve. The square marks represent the calculated $\delta\dot{q}/\delta\dot{w}$ term and the controller makes the system operated at the point where COP and $\delta\dot{q}/\delta\dot{w}$ are the same. Hence, the controller adjusts the heat rejection pressure so that the system becomes to be operated at the point where COP line and $\delta\dot{q}/\delta\dot{w}$ line crosses. In the figure, it is found that the maximum COP and operating point where the controller indicates are no exactly same

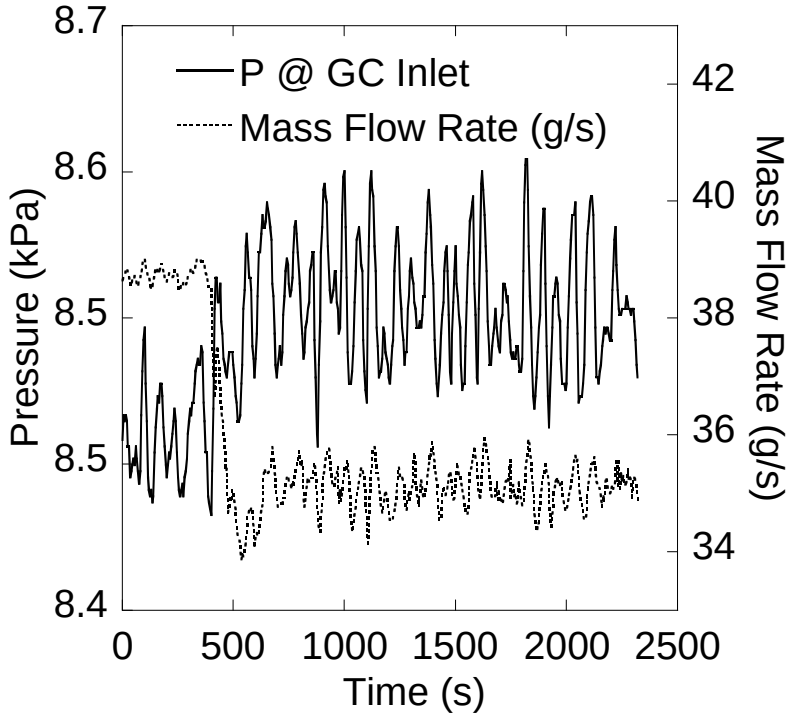

Fig. 4.8 Response of gas-cooler pressure and refrigerant mass flow rate when real time control starts at specified time ($T_{2nd,\,in}$: 27˚C)

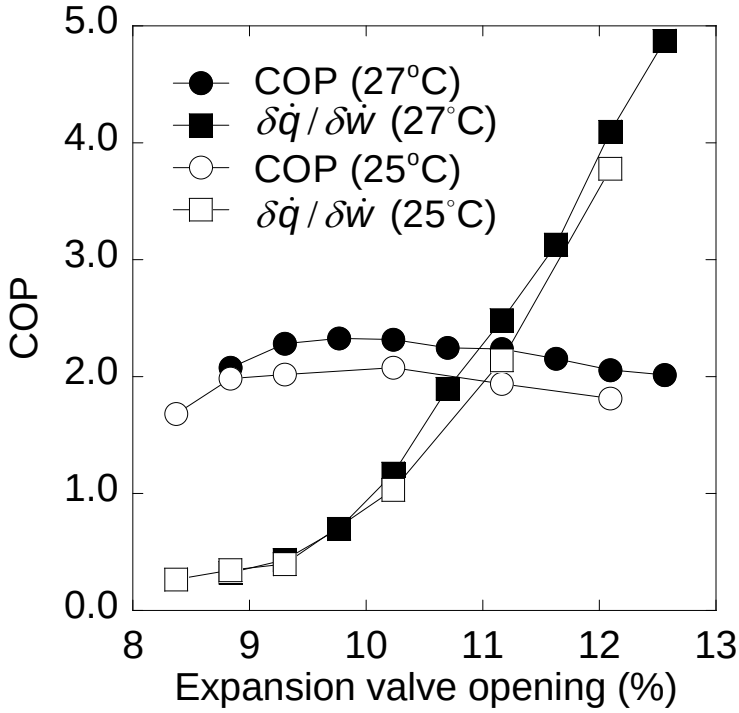

Fig. 4.9 Variation of COP and $\delta\dot{q}/\delta\dot{w}$ parameter with respect to change of expansion valve opening when the secondary fluid temperature at evaporator inlet is 27˚C and 25˚C

but it is biased from the optimal value. The bias is generated because the control method used the three assumptions which are stated in the previous chapter and the real system does not follow the assumptions.

Referring to the results, one can say that the controller adjusts the expansion valve opening to be slightly larger than its optimum value and the heat rejection pressure becomes lowered from its optimal value. The trend also can be stated that the calculated value of $\delta\dot{q}/\delta\dot{w}$ is lower than it should have been because the $\delta\dot{q}/\delta\dot{w}$ line will cross the COP line at the maximum COP point if the value of $\delta\dot{q}/\delta\dot{w}$ becomes higher than the presented values in the figures.

In this study, the reason of the bias will be investigated based on the theoretical analysis. Before carrying out the analysis of the experimental results, it should be noted that the energy balance makes the above control method valid regardless of the existence of an internal heat exchanger if all the above assumptions can be applied.

4.5 Discussion on the Factors Which Causes Inexact Estimation of the Optimal Point

4.5.1 Refrigerant temperature change at gas-cooler outlet

At first, the underestimation of the cooling capacity increment which is related with gas-cooler outlet state will be discussed. Equation (4.8) shows a very basic differential equation which can explain the enthalpy change caused by the change of pressure and temperature.

$$dh = \left.\frac{\partial h}{\partial P}\right|_T dP + \left.\frac{\partial h}{\partial T}\right|_P dT \tag{4.8}$$

As seen in Eq. (4.8), enthalpy is a state function of two variables while the first term ($\partial h/\partial P \cdot dP$) on the right side of the Eq. (4.8) was only considered in Eq. (4.2). Enthalpy change according to temperature change ($\partial h/\partial T \cdot dT$) was ignored and the controller underestimated the cooling capacity increment. By referring to Table 4.2, one can roughly compare the significance of the term $\partial h/\partial P \cdot dP$ and $\partial h/\partial T \cdot dT$ using the data obtained from the experiment when evaporator secondary fluid inlet temperature was 27˚C. Pressure and temperature change (δP and δT) at gas-cooler outlet was calculated between two nearby steady-states and each steady-state was obtained by changing expansion valve opening by step revolution (0.1 revolution, 0.465% of full scale revolution of the expansion valve) and partial differentiated terms ($\partial h/\partial P$ and $\partial h/\partial T$) were calculated using REFPROP 8.0 program.

The table says that the enthalpy difference caused by the temperature

Table 4.2 Parameters which affect enthalpy change

Exp. Open (%)	$\partial h/\partial P$	$\partial h/\partial T$	δP	δT	**(*A*)** $\partial h/\partial P \times \delta P$	**(*B*)** $\partial h/\partial T \times \delta T$	**(*A*+*B*)**	δh	**COP**
12.6	0.076	17.66	-	-	-	-	-	-	2.02
12.1	0.065	15.83	8.22	-0.17	0.53	2.65	3.18	3.41	2.06
11.6	0.050	13.07	30.95	-0.22	1.54	2.84	4.38	4.95	2.15
11.2	0.039	11.08	44.18	-0.17	1.73	1.83	3.56	3.99	2.24
10.7	0.031	9.37	46.75	-0.26	1.43	2.44	3.87	4.31	2.25
10.2	0.019	7.01	78.40	-0.81	1.50	5.71	7.21	8.49	2.32
9.8	0.011	5.35	103.19	-1.29	1.22	6.88	8.10	9.38	2.33
9.3	0.008	4.28	187.36	-1.60	1.42	6.85	8.26	9.37	2.28
8.8	0.006	3.83	267.52	-0.74	1.57	2.84	4.41	4.78	2.08

change (B) is larger than the pressure term (A) and this trend is stronger at near the optimal region. This is one of the most important reasons which make the underestimation of cooling capacity increment. To achieve higher efficiency with the controller, the temperature change should be considered. However, if gas-cooler is sufficiently large, it is expected that δT in the temperature change becomes negligible and the underestimation of the control method will be reduced.

Until now, with the above explanations, it might be concluded that the comparison of COP and $\delta\dot{q}/\delta\dot{w}$ is not meaningful because the temperature term ($\partial h/\partial T \cdot \delta T$) is dominant except the case when gas-cooler is much large. However, considering the case in which $\partial h/\partial P$ term is very large compared to $\partial w/\partial P$, appropriately larger specific cooling capacity than the increment of specific work can be obtained. If $\partial h/\partial T \cdot \delta T$ is larger than 0, more cooling capacity is added and COP will increase as upraising heat rejection pressure. Generally, $\partial h/\partial T \cdot \delta T$ term is larger than 0 because refrigerant mass flow rate decreases and gas-cooler effectiveness increase as expansion valve is closed.

This is presented in Fig. 4.10. The case which is presented in Fig. 4.10 is the same as the case of Table 4.2. $\Delta h/\Delta P$ represents the ratio of increased enthalpy to the increase of pressure according to the expansion valve

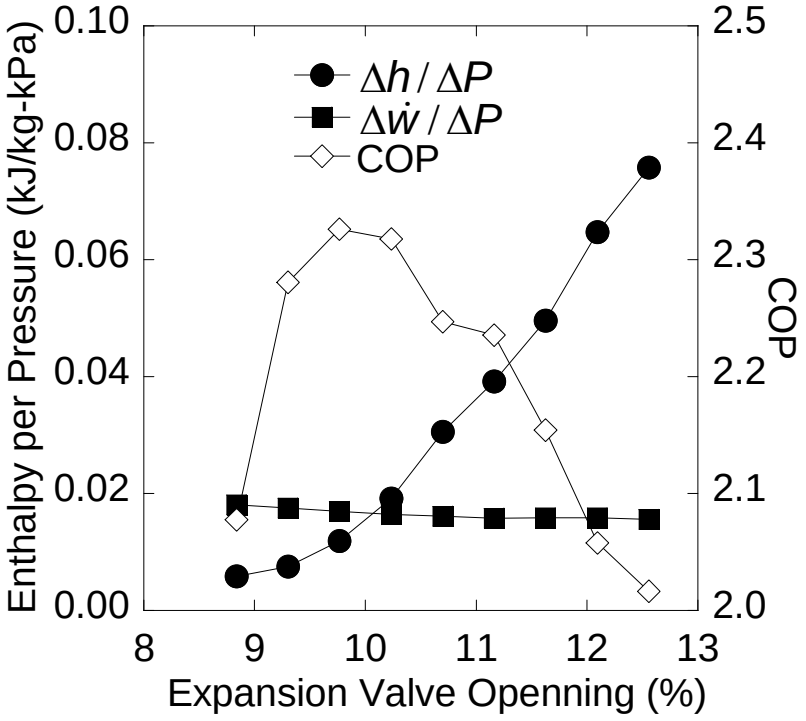

Fig. 4.10 Variation of $\partial h/\partial P$, $\partial w/\partial P$ and COP with respect to change of expansion valve opening ($T_{2nd,in}$: 27˚C)

opening change ($(h_{i+1}-h_i)/(P_{i+1}-P_i)$)and it can be regarded as a corresponding term of $\partial h/\partial P$. In ideal cases, the COP should be maximized at the point where the ratio of $\Delta h/\Delta P$ to $\Delta \dot{w}/\Delta P$ is the same with present COP and below this expansion valve opening, additional work is much greater than the cooling capacity increase, resulting in lowering the COP. However, with some reasons including the above, the figure shows that the maximum COP locates some biased point. Nevertheless, in the larger open region than 11.5% of opening, it obviously shows that COP is elevated with respect to close of expansion valve and $\Delta h/\Delta P$ is much larger than $\Delta \dot{w}/\Delta P$. In this aspect, it can be told that this real time control method helps a CO2 refrigeration system to avoid being operated with inadequately large expansion opening valve opening.

If gas-cooler size is extremely small and expansion valve opening is much closed, the situation presented in Fig. 4.11 can occur. That is, gas-cooler outlet state places where slope of isothermal line is very steep and in the region, the pressure term ($\partial h/\partial P \cdot \delta P$) in Eq. (4.8) will little change but the temperature term ($\partial h/\partial T \cdot \delta T$) will solely change. In this situation the real time control method can severely underestimate the specific cooling capacity increment and system operation condition can be far from its optimum. This is one of the intrinsic limits of the real time control method. However, the

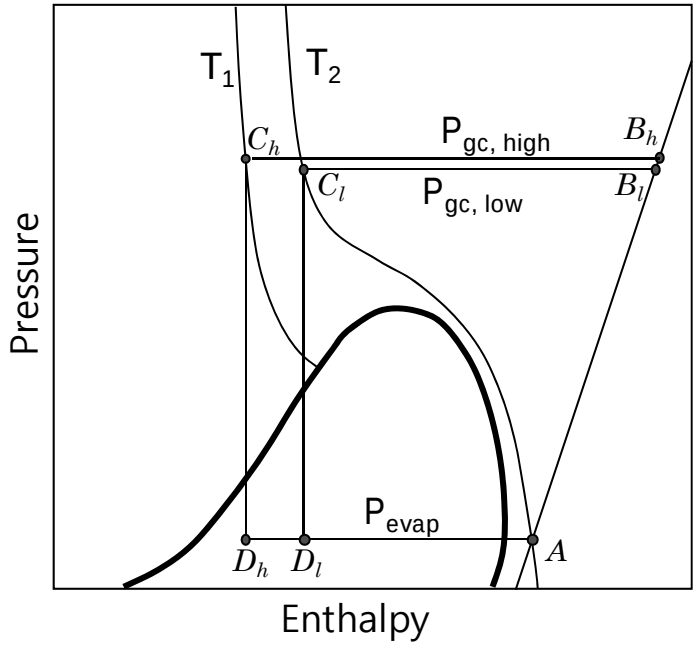

Fig. 4.11 Pressure-enthalpy diagram of a CO_2 refrigeration system with small gas-cooler

extreme case is not usual and with appropriately designed system, it is expected that the controller will show fairly good performance. Moreover, many of the variable frequency refrigeration system are used for part load operation and relatively large gas-cooler condition can be achieved. The bias effect of the control method will be reduced and the availability of the control method can be enhanced.

In the experiment the gas-cooler effectiveness was varied from 80 to 100% and 96% COP compared to the exact optimal COP was obtained using the real time controller (inlet water temperature of evaporator: 27˚C,). When the gas-cooler effectiveness ranged from 60 to 80%, 93% of the maximum COP was obtained (inlet water temperature of evaporator: 25˚C) and it is fairly acceptable performance. The gas-cooler effectiveness is presented in Fig. 4.12.

4.5.2 Evaporator pressure change

The control method suggested in this study also does not consider the change of evaporator pressure. If opening of an expansion valve is decreased without any other changes, the refrigerant mass flow rate is reduced and evaporator pressure becomes lowered. The lowered evaporator pressure enhances heat transfer in evaporator while the reduced mass flow rate

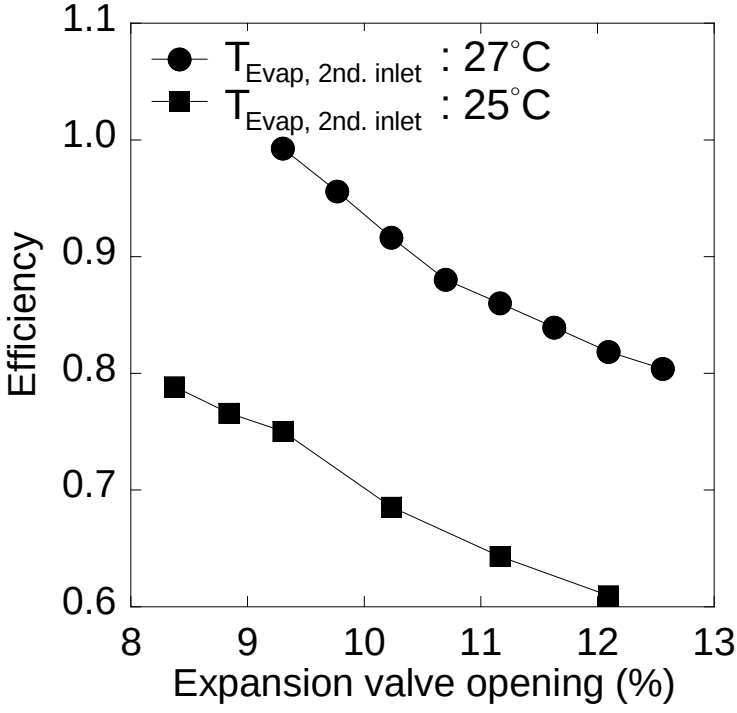

Fig. 4.12 Variation of gas-cooler efficiency with respect to change of expansion valve opening when the secondary fluid temperature at evaporator inlet is 27˚C and 25˚C

suppresses heat transfer. However, the impact of the decreased mass flow rate on the overall heat transfer coefficient becomes relatively small when refrigerant state in evaporator is two-phase state (Heo *et al*. 2013). This means the temperature difference term in Eq. (4.9) becomes larger while the overall heat transfer coefficient U does not decrease significantly. As a result, constant cooling capacity controller raises the evaporating pressure by decreasing compressor frequency to maintain the cooling capacity constant and the evaporating temperature does not decrease much.

$$\dot{Q}_{cool} = \int U(T_{2nd} - T_{ref})dA \tag{4.9}$$

Fig. 4.13 shows that the controlled evaporating temperature does not change much while the expansion valve opening is varied. Hence, the evaporator pressure does not vary much until refrigerant is superheated. Heat transfer characteristics in superheated vapor region become drastically worse and after occurrence of superheated vapor in evaporator, the capacity controller makes evaporator pressure to be lowered. The phenomenon can be found in Fig. 4.13. The occurrence of superheated region is represented by degree of superheat (DSH) at evaporator outlet and it is shown that the evaporator pressure decreases rapidly with increase of DSH at evaporator outlet.

The gas-cooler pressure, however, does not maintain the present pressure

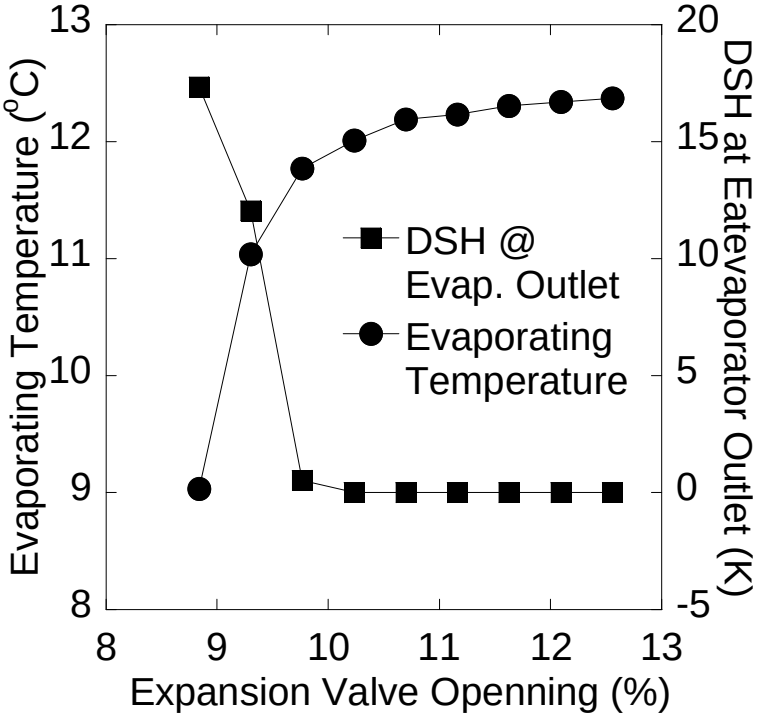

Fig. 4.13 Variation of evaporating temperature and DSH at compressor suction with respect to change of expansion valve opening ($T_{2nd,in}$: 27˚C)

as expansion valve is closed. Small mass flow rate causes rapider increase of refrigerant quality in evaporator and refrigerant amount which is contained in evaporator becomes reduced. The excessive refrigerant moves to gas-cooler and gas-cooler pressure arises as time goes by.

Near the optimal point, DSH at evaporator outlet is generally 0 and in this reason, evaporator pressure change is not so much significant compared with the pressure change of gas-cooler. Fig. 4.14 shows the absolute value of changed pressure when the expansion valve opening is changed by one step from the previous state. The below equation (Eq. 4.10) shows how is the changed pressure calculated.

$$\Delta P = \left| P_{i+1} - P_i \right| \tag{4.10}$$

At $i+1$ th expansion valve opening step, the i th pressure was subtracted and the result was defined as ΔP and presented in Fig. 4.14. As seen in the figure, the pressure change near the highest COP region of gas-cooler is 3.3 times larger than the pressure change of evaporator. However, it is obvious that the pressure change of evaporator gives substantial influence on the calculation of compressor work change. To neglect the evaporator pressure term in differential equation, the order of the value should be lower than that of the other terms but the degree of order of pressure change of evaporator does not seem smaller than that of gas-cooler. As a result, the negligence of

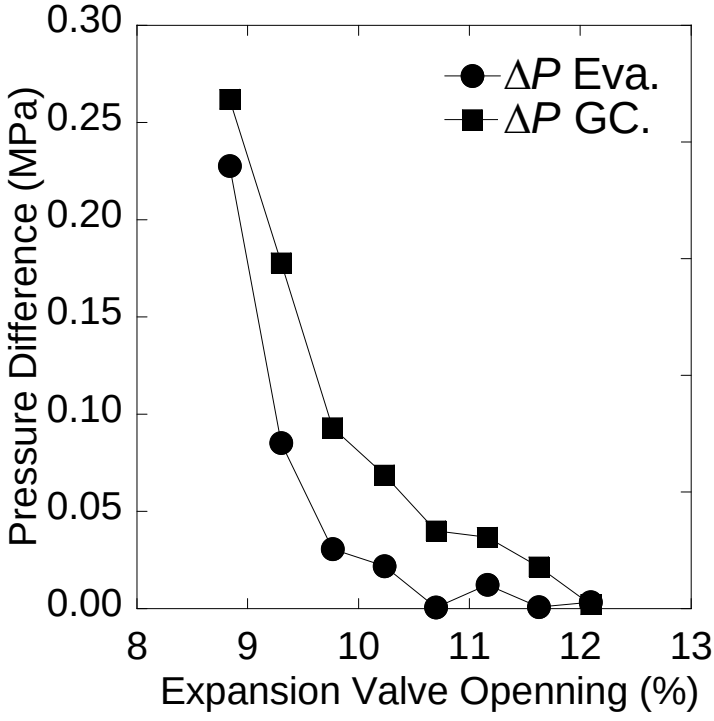

Fig. 4.14 Variation of gas-cooler pressure change, evaporator pressure change and COP with respect to change of expansion valve opening ($T_{2nd,in}$: 27˚C)

evaporator pressure change would yield some error of the controller.

In comprehensive aspects, neglecting evaporator pressure causes underestimation of increment of specific compressor work and it compensates underestimation of specific cooling capacity increment. Hence, in this situation, the negligence of evaporator pressure is helpful to reduce the bias caused by the underestimation of increment of cooling capacity. Nevertheless, in the final heat rejection control problem, it is necessary to devise a method which can consider the pressure change of evaporator and it is left to an assignment for future researches.

4.5.3 Enthalpy change at compressor suction

An internal heat exchanger is one of the key components for a CO_2 refrigeration system. The CO_2 refrigeration system in this study also has an internal heat exchanger and its effect was not included in the control method. Actually, it is too hard to consider the effect of an internal heat exchanger because the interactive behaviors among the system components are hard to estimate in a simple analytical method during the real time control. In this section, the effect of an internal heat exchanger and the change of refrigerant enthalpy at compressor suction on the control method will be analyzed.

In the suggested real time control method, it is assumed that the degree of

superheat (DSH) at compressor suction does not change in spite of the change of expansion valve opening. However, regardless of an internal heat exchanger, there is always a possibility of changing DSH at compressor suction. The increase of DSH at compressor suction induces higher specific enthalpy at gas-cooler inlet and the first law of thermodynamics guarantees more specific enthalpy change at the evaporator, which is shown in Fig. 4.15. Hence, DSH change at compressor suction can generate decrement or increment of specific cooling capacity which is undetectable by the real time controller.

Fig. 4.16 (a) shows steady-state pressure enthalpy diagrams with respect to different expansion valve opening when evaporator secondary fluid inlet temperature is 27˚C. Referring to the figure, one can recognize that the refrigerant enthalpy at high pressure side internal heat exchanger outlet does not significantly change in spite that the refrigerant enthalpy at gas-cooler outlet is substantially decreased as heat rejection pressure increases. Moreover, the enthalpy at high pressure side internal heat exchanger outlet even becomes slightly increases. The enthalpy increment at the high pressure side internal heat exchanger outlet possibly makes the specific cooling capacity decreased because the enthalpy at high pressure side internal heat exchanger outlet is directly the enthalpy at evaporator inlet. However,

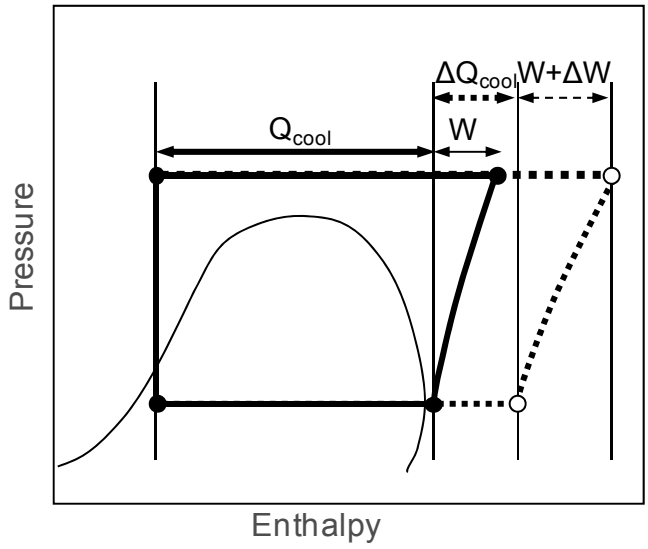

Fig. 4.15 Pressure-enthalpy diagram which represents relation between cooling capacity and enthalpy change at compressor suction

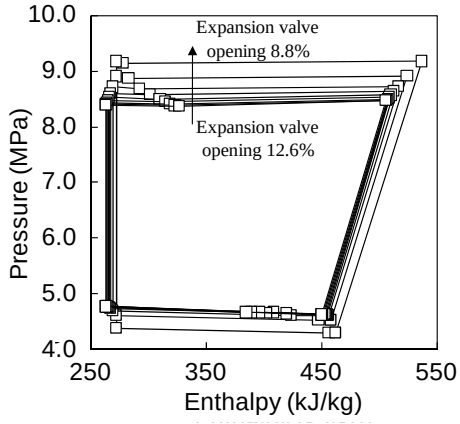

(a)

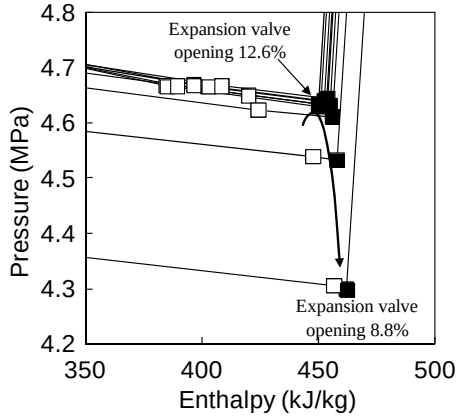

(b)

Fig. 4.16 Steady-state pressure-enthalpy diagram with respect to change of expansion valve opening (a) and its scaled-up graph near low pressure side internal heat exchanger inlet and compressor suction region (b) ($T_{2nd,in}$: 27˚C)

although the increment of the enthalpy at evaporator inlet, the specific cooling capacity was increased according to the close of the expansion valve because the refrigerant enthalpy at the evaporator outlet becomes increased.

With these results, it is important to confirm whether one can always achieve the increment of specific cooling capacity or not by reducing expansion valve opening. Prior to going further, one more basic principle should be regarded. It is that the gas-cooler outlet enthalpy decreases with respect to close of expansion valve and fortunately, this principle can easily be accepted. If then, the increment of specific cooling capacity can be affirmed when enthalpy at compressor suction does not decrease. The first law of thermodynamics ensures the above statement and it is presented in the following equations and inequalities (4.11).

$$\dot{q}_{heat} = h_{gc,in} - h_{gc,out}$$

$$\dot{q}_{cool} = h_{eva,out} - h_{eva,in}$$

$$\dot{w} = h_{gc,in} - h_{comp,suc}$$

$$\dot{q}_{cool} = \dot{q}_{heat} - \dot{w} = h_{comp,suc} - h_{gc,out}$$

$$\therefore \dot{q}_{cool,2} \geq \dot{q}_{cool,1}$$

when

$$h_{comp,suc,2} \geq h_{comp,suc,1} \quad \text{and} \quad h_{gc,out,2} \leq h_{gc,out,1} \tag{4.11}$$

Fig. 4.16 (b) shows the scaled up graph of Fig. 4.16 (a). It shows low pressure side internal heat exchanger inlet (white points) and compressor suction (black points) with respect to each step of the expansion valve opening and the figure says that there exists some extra specific cooling capacity increment. This situation is presented in Fig. 4.15. Hence, it should be investigated that how the compressor suction state changes.

The next step is analyzing how the system responds to the close of expansion valve. Fig. 4.17 is provided to help understanding the behavior of the refrigeration system. The solid line represents the original state before expansion valve opening is decreased and the dashed line represents hypothetically and sequentially divided processes of CO_2 refrigeration system which responds to the slight close of expansion valve. In any changed situation, total cooling capacity preserves its value because of capacity controller and Eq. (4.12) can be derived. The notation *h(A)* represents enthalpy at point A and *h(AB)* represents *h(B)-h(A)*.

$$(\dot{m} - \Delta\dot{m})h(E'F') = \dot{m}h(EF) \tag{4.12 a}$$

or

$$\frac{\Delta\dot{m}}{\dot{m}} = \frac{h(E'F') - h(EF)}{h(E'F')} \tag{4.12 b}$$

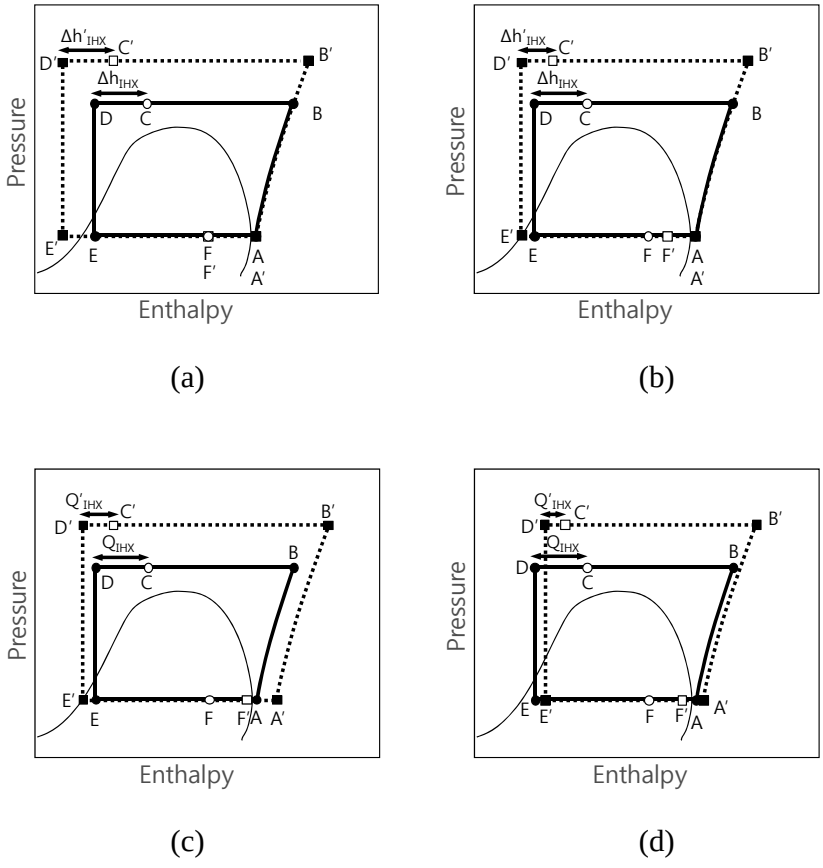

Fig. 4.17 Hypothetically divided processes of response of a CO_2 refrigeration system with small decrease of expansion valve opening

As expansion valve is closed, gas-cooler pressure starts to increase and gas-cooler outlet enthalpy becomes smaller. At this time, it is assumed that the point A and specific enthalpy change in internal heat exchanger preserve its present state ($h(A') = h(A)$, $P(A') = P(A)$, $h(D'C') = h(DC)$, $h(F'A') = h(FA)$). The situation is presented in Fig. 4.17 (a) and $h(F)$ does not vary. However, as increasing heat rejection pressure, specific heat capacity in high pressure side internal heat exchanger gets smaller and smaller and $T(C')$ becomes less or equal than $T(C)$. This situation leads reduce of $h(D'C')$ and the state can be represented as Fig. 4.17 (b). Until this, $h(A')$ is the same with $h(A)$ because the sole changed amount of heat transfer in internal heat exchanger is compensated by change of enthalpy at inlet and outlet of each side of internal heat exchanger.

An important factor which make $h(A')$ vary is specific cooling capacity ($h(E'F')$). If $h(E'F')$ becomes larger than $h(C'A)$ (Fig. 4.17 (c)) the first law of thermodynamics makes $h(A')$ increased. However, if $T(C)$ moves within the area near isothermal line and the effectiveness of internal heat exchanger is 100%, $h(A')$ does not vary because $T(A')$ does not vary (generally the low pressure side internal heat exchanger has less heat capacity). Eqs. (4.13) and (4.14) shows the above statement.

$$\begin{aligned}\varepsilon Q_{max,IHX} &= \varepsilon \dot{m}(h(P_{IHX,l,out}, T_{IHX,h,in}) - h(P_{IHX,l,in}, T_{IHX,l,in})) \\ &= \dot{m}(h(P_{IHX,l,out}, T_{IHX,l,out}) - h(P_{IHX,l,in}, T_{IHX,l,in}))\end{aligned} \tag{4.13}$$

$$\begin{aligned}&h(P_{IHX,l,out}, T_{IHX,l,out}) \\ &\quad = \varepsilon h(P_{IHX,l,out}, T_{IHX,h,in}) + (1-\varepsilon) h(P_{IHX,l,in}, T_{IHX,l,in})\end{aligned} \tag{4.14}$$

Hence, the enthalpy increment at evaporator outlet (*h(F')*) is compensated by the enthalpy decrement at high pressure side internal heat exchanger (*h(D')*) outlet and final state of the system can be represented by Fig. 4.17 (d).

On the other side, if *h(E'F')* becomes smaller than *h(C'A)* and the internal heat exchanger effectiveness is fairly small, *h(A')* can moves left resulting in smaller specific cooling capacity according to increase of heat rejection pressure. This result conflicts with the basic control principle. However, in general case, compressor frequency significantly decreases for keeping constant $UA\Delta T$ as referred in the chapter 3.2. (b), and the reducing of mass flow rate of refrigerant dominantly affects to determining *h(F)*. Hence, *h(E'F')* becomes larger than *h(C'A)* in general case.

If *h(F')* becomes any larger, the maximum specific heat transfer in lower pressure side internal heat exchanger decreases and it results in smaller enthalpy change in internal heat exchanger. This means smaller *h(D'C')* and *h(F'A')*. Then, the point *D'* and *E'* goes right and as *E'* moves right, it makes

easier for F' to moves right. After then, the maximum heat transfer amount of low pressure side internal heat exchanger

In Fig. 4.18, one can compare the enthalpy change at gas-cooler outlet with that at compressor suction in situation of one step change of expansion valve opening. The enthalpy difference between two steady-states was calculated by Eq. (4.15) and the evaporator secondary fluid inlet temperature was 27˚C.

$$\Delta h = \left| h_{i+1} - h_i \right| \tag{4.15}$$

In Fig. 4.18, the round mark represents enthalpy change at gas-cooler outlet and the square mark represents enthalpy change at compressor suction. Near the maximum COP region, the enthalpy change at gas-cooler outlet is about 7.4 times larger than that at compressor suction. However, as expansion valve opening becomes smaller, refrigerant enthalpy change at compressor suction becomes larger while gas-cooler outlet enthalpy change becomes smaller beyond some point. At small value of expansion valve opening, gas-cooler outlet temperature approaches to the secondary fluid inlet temperature very closely and slope of isothermal line at gas-cooler outlet goes steeper. Hence, gas-cooler outlet enthalpy does not decrease significantly. On the contrary, at pressure change in evaporator becomes larger at small value of expansion valve opening and enthalpy change at

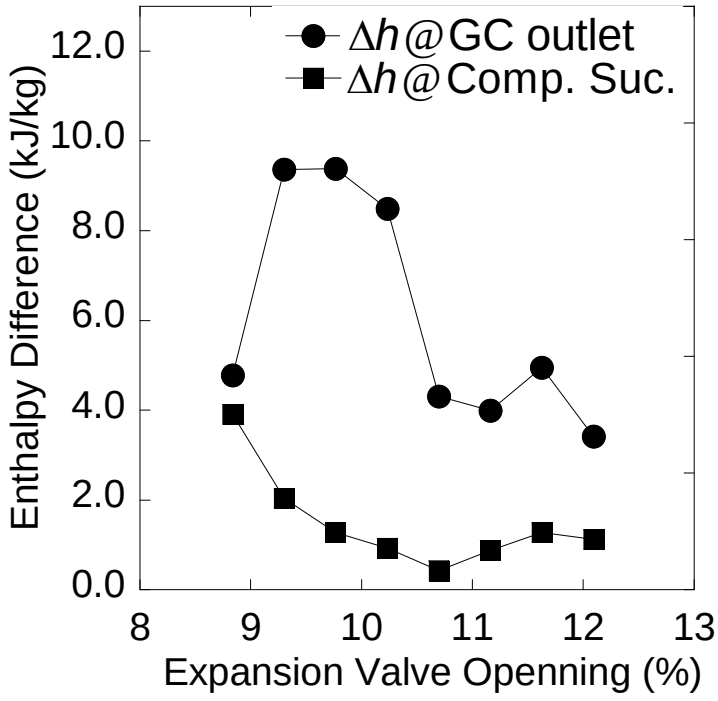

Fig. 4.18 Variation of enthalpy at gas-cooler outlet, compressor suction and COP with respect to change of expansion valve opening ($T_{2nd,in}$: 27˚C)

compressor suction becomes increased. However, this situation does not occur in near optimal region (refer to the previous section).

As a result, the real time controller might underestimate the cooling capacity increment. However, the evaporator pressure near optimal region does not change much and if a system adopts sufficiently large gas-cooler and internal heat exchanger, temperature at compressor suction will not change much according to the change of expansion valve opening and the enthalpy also will not change significantly. In this condition the proposed real time control method is expected to show a good performance.

4.6 Conclusion

In this paper, a real time heat rejection control method which does not require preliminarily obtained database or correlations was introduced. The introduced control method determines whether expansion valve opening must be closed or opened based on the calculations with the obtained data in real time.

The basic principles have descended from the old graphical method and the graphical method was modified to apply to a real time control system. The ratio of expected increment of cooling capacity and compression work

were calculated when slight close of expansion valve is assumed and the controller judges whether expansion valve should be closed or opened by comparing the calculated ratio and present COP in real time. Data acquisition system, property calculation process and PI control system were used to implement the control method. The real time control method was applied to a CO_2 refrigeration system with constant cooling capacity controller. It was shown that the system operates in a nearly optimal region with fairly acceptable controllability.

Some of the assumptions were applied to the establishment of the control method and the controller intrinsically cannot calculate the exact optimal operation point. In this study, three of the important factors which are related with the assumptions were investigated. The influences of temperature change at gas-cooler outlet, evaporator pressure change and change of enthalpy at compressor suction on the control method were analyzed. Among the presented factors, evaporator pressure change is not regarded as a critical problem. Near the optimal control region, refrigerant state at evaporator outlet is two-phase state and the constant cooling capacity controller keeps the evaporating pressure change in very limited range. The effect of refrigerant temperature change at gas-cooler outlet and enthalpy change at compressor suction are related with gas-cooler size and internal heat

exchanger size, respectively. In the analysis, if a system is equipped with sufficiently large heat exchangers, the controller is expected to operate well.

The newly introduced real time optimal control method for heat rejection pressure showed a fairly good performance in a real system. In this study, important analysis on the real time optimal control method was provided and it is expected that the study becomes a good guide for the subsequent studies related with the real time optimal control method.

Chapter 5. Concluding remarks

Recently, the problems of reducing energy consumption and using environmentally benign refrigerant have been raised with much of interest in refrigeration engineering field. In this study, a heat pump system for electric vehicle was investigated for enhancing heating capacity by utilizing vapor injection technique and novel controlling method for energy efficiency optimization of CO_2 refrigeration system was devised.

Vapor injection technique is one of the popular techniques which is used for a heat pump to enhance heating capacity in cold operating conditions. On the contrary to the fame of the technique, qualitative and comprehensive investigations on vapor injection technique are not presented much yet. Especially heat pump for electric vehicle is kind of developing apparatus and it is not studied widely in the refrigeration fields. In this study, a heat pump system to which vapor injection is applied was investigated for electric vehicle. The some of the special characteristics of heat pump system for vehicle was considered. Comparatively small condenser size and the same temperature conditions of indoor and outdoor side were given to the experimental system.

In the experimental results, it was concluded that as controlling vapor

injection refrigerant amount and charging appropriately sufficient refrigerant charge, one can obtain substantially increased heating capacity with less decrease of COP. Additionally, because the system has small condenser size, condenser pressure influences heating capacity much and it can be told that problem of controlling condenser pressure is kind of an important issue. Followed the experimental investigation, numerical investigation was performed. Through the investigation, it was revealed that there exists optimal condenser pressure which provides large heating capacity with the smallest COP degrade. It also showed that the injection hole of the vapor injection compressor restricts the increment of heating capacity within some amount and it should be expanded as possible as leakage does not occur.

A CO_2 refrigeration system recently attracts much of attention in aspect of using environmentally benign refrigerant which has 0 ODP and very low GWP. However its efficiency control is somewhat complicated problem because CO_2 refrigeration system operates in trans-critical conditions. Novel control method for controlling COP of CO_2 refrigeration system was devised in this study and it was validated through experiment. Assuming an ideal CO_2 refrigeration system, the ratio of cooling capacity increment to the compression work increment was estimated and it was compared with COP. When COP and the ratio is the same, the system was considered to have the

maximum COP. The devised control method is not theoretically perfect but showed acceptable performance. Some of the limitations and causes of generating performance degrade were analyzed in the study.

It is expected that these studies is able to provide much useful information on reducing energy consumption by adopting vapor injection technique to vehicle heat pump system and using CO_2 refrigeration system with higher energy efficiency.

References

Baek, C., Heo, J., Jung, J., Cho, H., Kim, Y., 2013. Optimal control of the gas-cooler pressure of a CO_2 heat pump using EEV opening and outdoor fan speed in the cooling mode. International Journal of Refrigeration.

Beeton, W.L., Pham, H.M., 2003. Vapor-injected scroll compressors. ASHRAE journal 45, 22-27.

Bertsch, S.S., Groll, E.A., 2008. Two-stage air-source heat pump for residential heating and cooling applications in northern U.S. climates. International Journal of Refrigeration 31, 1282-1292.

Cecchinato, L., Chiarello, M., Corradi, M., Fornasieri, E., Minetto, S., Stringari, P., Zilio, C., 2009. Thermodynamic analysis of different two-stage transcritical carbon dioxide cycles. International Journal of Refrigeration 32, 1058-1067.

Cecchinato, L., Corradi, M., Cosi, G., Minetto, S., Rampazzo, M., 2012. A real-time algorithm for the determination of R744 systems optimal high pressure. International Journal of Refrigeration 35, 817-826.

Cecchinato, L., Corradi, M., Minetto, S., 2010. A critical approach to the determination of optimal heat rejection pressure in transcritical systems. Applied Thermal Engineering 30, 1812-1823.

Chen, Y., Gu, J., 2005. The optimum high pressure for CO_2 transcritical refrigeration systems with internal heat exchangers. International Journal of Refrigeration 28, 1238-1249.

Chen, Y., Halm, N.P., Groll, E.A., Braun, J.E., 2002. Mathematical modeling of scroll compressors - part I: compression process modeling. International Journal of Refrigeration 25, 731-750.

Chi, J., Didion, D., 1982. A simulation model of the transient performance of a heat pump. International Journal of Refrigeration 5, 176-184.

Cho, H., Ryu, C., Kim, Y., Kim, H.Y., 2005. Effects of refrigerant charge amount on the performance of a transcritical CO_2 heat pump. International Journal of Refrigeration 28, 1266-1273.

Cho, I.Y., Bin Ko, S., Kim, Y., 2012. Optimization of injection holes in symmetric and asymmetric scroll compressors with vapor injection. International Journal of Refrigeration 35, 850-860.

Corberán, J.M., Martínez, I.O., Gonzálvez, J., 2008. Charge optimisation study of a reversible water-to-water propane heat pump. International Journal of Refrigeration 31, 716-726.

Domanski, P.A., 1995. Theoretical evaluation of the vapor compression cycle with a liquid-line/suction-line heat exchanger, economizer, and ejector. National Institute of Standards and Technology.

He, S., Guo, W., Wai, E.W., 2006. Northern china heat pump application with the digital heating scroll compressor. Proc. Int. Refrigeration and Air Conditioning Conference, West Lafayette, IN, USA.

Heo, J., Lee, H., Yun, R., 2013. Two-phase Flow Boiling and Condensation Heat Transfer Characteristics of Natural Refrigerants: Review. International Journal of Air-Conditioning and Refrigeration 21, 133003.

Hwang, Y., Radermacher, R., 1998. Theoretical evaluation of carbon dioxide refrigeration cycle. HVAC&R Research 4, 245-263.

Inokuty, H., 1923. Approximate graphical method of finding compression pressure of CO_2 refrigerant machine for max. coefficient of performance, 92th Japan Society of Mechanical Engineers.

Kauf, F., 1999. Determination of the optimum high pressure for transcritical CO_2-refrigeration cycles. International Journal of Thermal Sciences 38, 325-330.

Kim, M.S., Kim, M.S., 2012. An On-line Control Method of Optimal Heat Rejection Pressure for CO_2 Refrigeration Cycle, 10th IIR Gustav Lorentzen Conference 2012, Delft, The Netherlands.

Kim, S.G., Kim, Y.J., Lee, G., Kim, M.S., 2005. The performance of a transcritical CO2 cycle with an internal heat exchanger for hot water heating. International Journal of Refrigeration 28, 1064-1072.

Lee, J.S., Kim, M.S., Kim, M.S., 2014. Studies on the performance of a CO2 air conditioning system using an ejector as an expansion device. International Journal of Refrigeration 38, 140-152.

Lemmon, E., Huber, M., McLinden, M., 2007. REFPROP 8.0, NIST Standard reference database.

Liao, S., Zhao, T., Jakobsen, A., 2000. A correlation of optimal heat rejection pressures in transcritical carbon dioxide cycles. Applied Thermal Engineering 20, 831-841.

Liu, T., Liu, Z.Q., 2004. Study on Geometry Theory of Trigonometric-Curve Modification of Scroll Profile for Scroll Compressor. Proc. Int. Compressor Enginerring Conference.

Liu, Y., Hung, C., Chang, Y., 2009. Mathematical model of bypass behaviors used in scroll compressor. Applied Thermal Engineering 29, 1058-1066.

Liu, Z., Du, G., Qi, Z., Gu, J., 1994. The conjugacy analysis of modified part of scroll profiles. Proc. International Compressor Engineering Conference.

Liu, Z., Du, G., Yu, S., Wang, M., 1992. The Graphic Method of Modified Wrap Scroll Compressor. Proc. Int. Compressor Enginerring Conference.

Ma, G.-Y., Chai, Q.-X., 2004. Characteristics of an improved heat-pump cycle for cold regions. Applied Energy 77, 235-247.

Ma, G.-Y., Zhao, H.-X., 2008. Experimental study of a heat pump system with flash-tank coupled with scroll compressor. Energy and Buildings 40, 697-701.

Moffat, R.J., 1988. Describing the uncertainties in experimental results. Experimental thermal and fluid science 1, 3-17.

Morini, G.L., 2004. Single-phase convective heat transfer in microchannels: a review of experimental results. International Journal of Thermal Sciences 43, 631-651.

Neksså, P., Rekstad, H., Zakeri, G.R., Schiefloe, P.A., 1998. CO_2 heat pump water heater: characteristics, system design and experimental results. International Journal of Refrigeration 21, 172-179.

Pitla, S.S., Groll, E.A., Ramadhyani, S., 2002. New correlation to predict the heat transfer coefficient during in-tube cooling of turbulent supercritical CO2. International Journal of Refrigeration 25, 887-895.

Rozhentsev, A., Wang, C.-C., 2001. Some design features of a CO2 air conditioner. Applied Thermal Engineering 21, 871-880.

Sarkar, J., Bhattacharyya, S., Gopal, M.R., 2004. Optimization of a transcritical CO_2 heat pump cycle for simultaneous cooling and heating applications. International Journal of Refrigeration 27, 830-838.

Siddharth, J., Gaurav, J., Clark W, B., 2004. Vapor injection in scroll compressors. Proc. Int. Compressor Enginerring Conference, West Lafayette, IN, USA.

Vjacheslav, N., Rozhentsev, A., Wang, C.C., 2001. Rationally based model for evaluating the optimal refrigerant mass charge in refrigerating machines. Energy Conversion and Management 42, 2083-2095.

Wang, B., Li, X., Shi, W., Yan, Q., 2006. Effects of refrigerant injection on the scroll compressor. Proc. Int. Compressor Enginerring Conference, West Lafayette, IN, USA.

Wang, B., Li, X., Shi, W., Yan, Q., 2007. Design of experimental bench and internal pressure measurement of scroll compressor with refrigerant injection. International Journal of Refrigeration 30, 179-186.

Wang, X., Hwang, Y., Radermacher, R., 2009. Two-stage heat pump system with vapor-injected scroll compressor using R410A as a refrigerant. International Journal of Refrigeration 32, 1442-1451.

Wang, Z., Gong, Y., Wu, X., Zhang, W., Lu, Y., 2013. Thermodynamic Analysis and Experimental Research of Transcritical CO_2 Cycle with Internal Heat Exchanger and Dual Expansion. International Journal of Air-Conditioning and Refrigeration 21.

Xu, X., Hwang, Y., Radermacher, R., 2011. Refrigerant injection for heat pumping/air conditioning systems: Literature review and challenges discussions. International Journal of Refrigeration 34, 402-415.

Yokoyama, R., Shimizu, T., Ito, K., Takemura, K., 2007. Influence of ambient temperatures on performance of a CO_2 heat pump water heating system. Energy 32, 388-398.

Zehnder, M., Favrat, D., Hohl, H., Olivier, C., Perevozchikow, M., 2002. High performance air-water heat pump with extended application range for residential heating. 7th International Energy Agency, Heat Pump Conference, Beijing 2, 702.

Zhang, W.-J., Zhang, C.-L., 2011. A correlation-free on-line optimal control method of heat rejection pressures in CO_2 transcritical systems. International Journal of Refrigeration 34, 844-850.

국 문 초 록

근래 에너지 소비의 효율적 활용에 많은 관심이 모아지고 있으며 합성냉매가 환경에 미치는 영향에 대한 우려도 커지고 있다. 이러한 상황에서 미래의 친환경 수송수단으로 배기가스 등의 문제가 없고 보다 효율적이 에너지의 사용이 가능한 전기자동차가 차세대 수송수단으로 고려되고 있다. 그러나 전기자동차는 엔진과 같은 폐열원이 없어 난방문제를 따로 해결해야 하며 난방을 단순 전열기를 이용하여 수행하게 될 경우 동력으로 사용해야 하는 전기의 양이 크게 감소하여 열펌프를 적용하는 방안이 대두되고 있다. 하지만 크기의 제한조건이 있는 자동차의 특성 상 압축기의 크기에도 제한이 있게 되어 행정체적의 부족문제를 야기하고 결과적으로 겨울철 난방용량이 부족하게 된다. 가정용이나 상업용 열펌프 시스템에서는 이러한 문제를 해결하기 위하여 기상냉매 주입기술이 개발되어 사용되고 있으나 현재까지 자동차용 열펌프 시스템에 적용된 기상냉매 주입기술은 많이 연구되어있지 않은 상황이다. 본 연구에서는 기상냉매 주입기술을 적용하는 데 있어서 자동차 열펌프 시스템의 운전조건을 고려하여 난방용량을 최대화하고 에너지 이용효율을 높이는 방향으로 시스템 설계 및 제어를 수행하기 위해 실험적 연구와 해석적 연구를 수행하였으며 이를 통하여 기상냉매 주입기술의 자동차 열펌프에의 적용가능성을 확인하였고 각 제어변수 및 냉매 충전량이 난방용량에 미치는 영향을 분석하였다. 또한 본 연구에서는 기상냉매 주입기술에 관한 연구와는 별개로 최근 친환경 냉매로 각광받고 있는 이산화탄소 냉매 이용 냉방시스템의 최적 제어에 관한 연구를 수행하였다. 이산화탄소는 오존층 파괴효과가 전혀 없고 지구온난화에 미치는 영향이 상대적으로 매우 미미하여 그 활용이 기대되고 있으나 고압부가 초 임계 상태로 작동하게 되어 최적고압제어에 어려움이 있다. 본 연구에서는 이상적인

이산화탄소 냉방 시스템을 가정하여 미소 압력 상승 시 기대되는 냉방용량의 상승과 압축일의 상승을 예측하여 이의 비율을 현재 COP 와 비교하는 방식으로 최적의 고압을 실시간으로 찾는 최적고압제어방법을 제시하였다. 실험적으로 제시된 제어방법을 검증하여 만족할만한 수준의 성능을 보이는 것을 확인하였으며 이상적인 냉방시스템을 가정하는 데서 오는 몇 가지 중요한 오차의 원인들을 분석하였다. 본 연구에서 제시된 실험 및 해석 결과들이 추후 기상냉매 주입방식 열펌프의 연구 및 이산화탄소 냉방시스템의 개발에 상당한 도움이 될 것으로 기대되며 이를 통하여 에너지 이용의 효율성 향상 및 친환경 냉매의 사용이 보다 쉬워질 것으로 예상된다.

주요어: 기상냉매 주입방식, 열펌프, 이산화탄소 냉매, 에너지효율, 난방용량

학 번: 2010-30791